

79P

5101-280
Flat-Plate
Solar Array Project

DOE/JPL-1012-113
Distribution Category UC-63b

2610

Environmental Tests of Metallization Systems for Terrestrial Photovoltaic Cells

Paul Alexander, Jr.

(JPL-Publ-85-86)	ENVIRONMENTAL TESTS OF	N86-25045
METALLIZATION SYSTEMS FOR TERRESTRIAL		
PHOTOVOLTAIC CELLS (Jet Propulsion Lab.)		
79 p HC A05/MF A01	CSCL 10A	Unclas
		G3/44 43381

December 31, 1985

Prepared for
U.S. Department of Energy
Through an Agreement with
National Aeronautics and Space Administration
by
Jet Propulsion Laboratory
California Institute of Technology
Pasadena, California

JPL Publication 85-86

5101-280
Flat-Plate
Solar Array Project

DOE/JPL-1012-113
Distribution Category UC-63b

Environmental Tests of Metallization Systems for Terrestrial Photovoltaic Cells

Paul Alexander, Jr.

December 31, 1985

Prepared for
U.S. Department of Energy
Through an Agreement with
National Aeronautics and Space Administration
by
Jet Propulsion Laboratory
California Institute of Technology
Pasadena, California

JPL Publication 85-86

Prepared by the Jet Propulsion Laboratory, California Institute of Technology, for the U.S. Department of Energy through an agreement with the National Aeronautics and Space Administration.

The JPL Flat-Plate Solar Array Project is sponsored by the U.S. Department of Energy and is part of the Photovoltaic Energy Systems Program to initiate a major effort toward the development of cost-competitive solar arrays.

This report was prepared as an account of work sponsored by an agency of the United States Government. Neither the United States Government nor any agency thereof, nor any of their employees, makes any warranty, express or implied, or assumes any legal liability or responsibility for the accuracy, completeness, or usefulness of any information, apparatus, product, or process disclosed, or represents that its use would not infringe privately owned rights.

Reference herein to any specific commercial product, process, or service by trade name, trademark, manufacturer, or otherwise, does not necessarily constitute or imply its endorsement, recommendation, or favoring by the United States Government or any agency thereof. The views and opinions of authors expressed herein do not necessarily state or reflect those of the United States Government or any agency thereof.

This publication reports on work done under NASA Task RE-152, Amendment 66, DOE / NASA IAA No. DE-AI01-76ET20356.

ABSTRACT

Seven different solar cell metallization systems were subjected to temperature cycling tests and humidity tests. Temperature cycling excursions were -50°C to 150°C per cycle. Humidity conditions were 70°C at 98% relative humidity. The seven metallization systems were: (1) Ti/Ag, (2) Ti/Pd/Ag, (3) Ti/Pd/Cu, (4) Ni/Cu, (5) Pd/Ni/Solder, (6) Cr/Pd/Ag, and (7) Thick Film Ag.

All of the seven metallization systems showed slight to moderate decreases in cell efficiencies after subjection to 1000 temperature cycles. Six of the seven metallization systems also evidenced slight increases in cell efficiencies after moderate numbers of cycles, generally less than 100 cycles. The copper-based systems showed the largest decrease in cell efficiencies after temperature cycling.

All of the seven metallization systems showed moderate to large decreases in cell efficiencies after 123 days of humidity exposure. The copper-based systems again showed the largest decrease in cell efficiencies after humidity exposure.

Graphs of the environmental exposures versus cell efficiencies are presented for each of the metallization systems, as well as environmental exposures versus fill factors or series resistance.

ACKNOWLEDGMENTS

Acknowledgments are extended to ASEC Corp. for fabricating the test cells, and to Jerry Stebbins, Lee Midling, and Ken Gray of the JPL Process Research Laboratory who conducted the environmental tests and generated the cell I-V data. Acknowledgments are also extended to Ron Williams for his help in editing this document.

PRECEDING PAGE BLANK NOT FILMED

PAGE IV INTENTIONALLY BLANK

CONTENTS

I.	INTRODUCTION	1-1
II.	PROCESSING OF SPECIMEN CELLS	2-1
III.	DISCUSSION OF METALLIZATION SYSTEMS	3-1
IV.	TEST EQUIPMENT	4-1
V.	TEST PROGRAM	5-1
VI.	TEST RESULTS	6-1
	A. I-V CHARACTERISTICS AFTER ENVIRONMENTAL EXPOSURE	6-1
	B. SECONDARY ION MASS SPECTROMETRY EVALUATION	6-27
	C. I-V CURVES OF TEMPERATURE CYCLING AND HUMIDITY EXPOSURE TESTS	6-29
VII.	DISCUSSION OF RESULTS	7-1
	A. OVERVIEW	7-1
	B. TEMPERATURE CYCLING TESTS	7-1
	C. DISCUSSION OF HUMIDITY TESTS	7-3
VIII.	REFERENCES	8-1
IX.	SELECTED BIBLIOGRAPHY	9-1
	APPENDIX	A-1

Figures

4-1.	Temperature and Humidity Chamber	4-2
4-2.	Temperature Cycling Chamber	4-3
4-3.	I-V Test Equipment, Light Source	4-4
4-4.	I-V Test Equipment, Data Printout	4-5
6-1.	Control Cells (No Environmental Exposures) for Ti/Ag, Ti/Pd/Ag, Ti/Pd/Cu, Ni/Cu, Pd/Ni/Solder, Cr/Pd/Ag and Thick Film Ag Paste	6-3
6-2.	Control Cells, After Temperature Cycling, and After Humidity Exposure, Ti/Ag (a, b and c)	6-4

6-3.	Control Cells, 40x, After Temperature Cycling, and After Humidity Exposure, Ti/Pd/Ag (a, b and c)	6-6
6-4.	Control Cells, 40x, After Temperature Cycling, and After Humidity Exposure, Ti/Pd/Cu (a, b and c)	6-8
6-5.	Control Cells, 40x, After Temperature Cycling, and After Humidity Exposure, Ni/Cu (a, b and c)	6-10
6-6.	Control Cells, 16x, After Temperature Cycling, and After Humidity Exposure, Pd/Ni/Solder (a, b and c)	6-12
6-7.	Control Cells, 40x, After Temperature Cycling, and After Humidity Exposure, Cr/Pd/Ag (a, b and c)	6-14
6-8.	Control Cells, 40x, After Temperature Cycling, and After Humidity Exposure, Thick Film Ag Paste (a, b and c)	6-16
6-9.	Temperature Cycling: Efficiency Versus Number of Cycles for Seven Metallization Systems	6-18
6-10.	Temperature Cycling: Percent Change in Efficiency Versus Number of Cycles for Seven Metallization Systems	6-18
6-11.	Temperature Cycling: Efficiency and Fill Factor Versus Number of Cycles, Ti/Ag	6-19
6-12.	Temperature Cycling: Efficiency and Fill Factor Versus Number of Cycles, Ti/Pd/Ag	6-19
6-13.	Temperature Cycling: Efficiency and Fill Factor Versus Number of Cycles, Ti/Pd/Cu	6-20
6-14.	Temperature Cycling: Efficiency and Fill Factor Versus Number of Cycles, Ni/Cu	6-20
6-15.	Temperature Cycling: Efficiency and Fill Factor Versus Number of Cycles, Pd/Ni/Solder	6-21
6-16.	Temperature Cycling: Efficiency and Fill Factor Versus Number of Cycles, Cr/Pd/Ag	6-21
6-17.	Temperature Cycling: Efficiency and Fill Factor Versus Number of Cycles, Thick Film Ag Paste	6-22
6-18.	Humidity Tests: Efficiency Versus Number of Days Exposure For All Seven Metallization Systems	6-22
6-19.	Humidity Tests: Percent Change in Efficiency Versus Number of Days Exposure For All Seven Metallization Systems	6-23

6-20.	Humidity Tests: Efficiency and Series Resistance Versus Number of Days Exposure, Ti/Ag	6-23
6-21.	Humidity Tests: Efficiency and Series Resistance Versus Number of Days Exposure, Ti/Pd/Ag	6-24
6-22.	Humidity Tests: Efficiency and Series Resistance Versus Number of Days Exposure, Ti/Pd/Cu	6-24
6-23.	Humidity Tests: Efficiency and Series Resistance Versus Number of Days Exposure, Ni/Cu	6-25
6-24.	Humidity Tests: Efficiency and Series Resistance Versus Number of Days Exposure, Pd/Ni/Solder	6-25
6-25.	Humidity Tests: Efficiency and Series Resistance Versus Number of Days Exposure, Cr/Pd/Ag	6-26
6-26.	Humidity Tests: Efficiency and Series Resistance Versus Number of Days Exposure, Thick Film Ag Paste	6-26
6-27.	Sample of the SIMS Profile Data	6-28
6-28.	I-V Curves of Temperature Cycling Test, Selected Sample, Ti/Pd/Cu	6-31
6-29.	I-V Curves of Temperature Cycling Test, Selected Sample, Ti/Pd/Ag	6-33
6-30.	I-V Curves of Humidity Exposure Test, Selected Sample, Ti/Pd/Cu	6-35
6-31.	I-V Curves of Humidity Exposure Test, Selected Sample, Ti/Pd/Ag	6-37

Tables

2-1.	Metallization Processing for Each Metallization System	2-2
3-1.	Block IV Metallization Systems	3-2
5-1.	Temperature Cycling Tests	5-1
5-2.	Humidity Exposure Tests	5-1
6-1.	Summary of the Results for Temperature and Humidity Exposure Tests	6-2
6-2.	Data for I-V Curves of Temperature Cycling Test, Selected Sample, Ti/Pd/Cu	6-30

6-3.	Data for I-V Curves of Temperature Cycling Test, Selected Sample, Ti/Pd/Ag	6-32
6-4.	Data for I-V Curves of Humidity Exposure Test, Selected Sample, Ti/Pd/Cu	6-34
6-5.	Data for I-V Curves of Humidity Exposure Test, Selected Sample, Ti/Pd/Ag	6-36

SECTION I

INTRODUCTION

The Flat-Plate Solar Array (FSA) Project was formed at the Jet Propulsion Laboratory (JPL) in 1975 under the sponsorship of the U.S. Department of Energy (DOE). The objective of the project was to reduce the cost of making solar cells to the point at which photovoltaic power would be cost-competitive with electrical power generated by fossil fuels. The cost goal for making terrestrial solar cells was established at \$0.70/watt (1980 dollars), a drastic reduction from over \$100/watt for space cell fabrication. This very severe cost reduction goal generated a re-thinking of the entire fabrication process, starting with the manufacture of solar grade silicon material, through silicon sheet formation, through cell processing, and through solar module fabrication. The terrestrial solar cell evolved from this re-thinking and is a slightly different species than the space solar cell. The silicon material, the silicon sheet, the solar cell processing and module fabrication for terrestrial application evolve from different fabrication techniques than space cell fabrication.

In the very important area of contact metallization of terrestrial solar cells, cheaper metals and new ways for applying them were pursued. The expensive vacuum evaporated titanium-palladium-silver metallization system, long (and still) the dominant, almost exclusive metallization system in space solar cells because of its very excellent performance properties, has given way in terrestrial applications to solder-based metallization systems, thick film metallization systems and copper based metallization systems, mostly because of their cheaper costs. Metal deposition by vacuum evaporation has given way to solder dipping, thick film printing and plating. Again, this is because of cheaper costs.

The literature on testing of solar cell metallization systems deals almost entirely with titanium-silver and titanium-palladium-silver metallization systems. This is because the early space cells, going back to the early 1960s, received considerable attention and funding to evaluate these two systems. The Ti/Ag system gave way to the Ti/Pd/Ag when it was determined that the addition of palladium helped the system against moisture ingress and improved cell performance degradation under humidity conditions. The Ti/Pd/Ag metallization system is, and has been for over 20 years, the dominant metallization system for space solar cells, and is also the "standard of comparison" in terrestrial cell work.

In this work seven metallization systems were selected and tested for terrestrial application: (1) Ti/Ag, (2) Ti/Pd/Ag, (3) Ti/Pd/Cu, (4) Ni/Cu, (5) Pd/Ni/Solder, (6) Cr/Pd/Ag, and (7) a Thick Film Ag paste. The tests conducted were very straightforward, similar to those found in the literature on testing. It was the intent of this program to evaluate these different metallization systems (as contrasted with qualifying such systems) and to assess the relative sensitivities of these metallization systems to the two most commonly tested environments, temperature cycling and humidity exposure. It is hoped that the data collected and described in this test program will add to the body of literature on environmental testing of solar cell metallization systems.

SECTION II

PROCESSING OF SPECIMEN CELLS

All cells used in this test program were from the same lot and processed as one lot through front and back junction formation. The starting material was 3 in. diameter, chemically polished, 12 mils thick, 2 ohm-cm, p-type, Czochralski (Cz) grown silicon with (100) orientation. The wafers were masked with SiO₂ using a low temperature, chemical vapor deposition process. The back P+ layer was first formed by boron nitride diffusion followed by the front N layer (0.3 μm deep) which was diffused using a POCl₃ source. The sheet resistance of the N layer surface was approximately 30 ohms/square. The silicon oxide layer, formed during diffusion, was removed by an HF dip. This procedure eliminated process variations in the front and back junctions since the junctions were all formed together for all seven metallization groups.

After the front and back junctions were formed, all of the 3 in. diameter cells were cut into 2 x 2 cm size blanks and equally divided into seven different metallization groups. Again, to eliminate as many process variables as possible, six of the seven metallization groups were metallized by vacuum evaporation through a shadow mask. The seventh group was metallized by screen printing. After completion of each metallization process, all of the cells were coated with Multilayer Antireflective (MLAR) coating and tested at Air Mass 1 (AM1), 28°C.

Table 2-1 presents the metallization process information on the seven metallization groups.

Table 2-1. Metallization Processing for Each Metallization System

Metallization System	Process
Ti/Ag	Evaporate the following: Ti (1000 Å) and Ag (3 μm), on both front and back sides, followed by 400°C, 10 min sintering in N ₂
Ti/Pd/Ag	Evaporate the following: Ti (1000 Å), Pd (500 Å) and Ag (3 μm), on both front and back sides, followed by 400°C, 10 min sintering in N ₂
Ti/Pd/Cu	Evaporate the following: Ti (1000 Å), Pd (500 Å) and Cu (2 μm), on both front and back sides, followed by 325°C, 10 min sintering in forming gas (10% H ₂ and 90% N ₂)
Ni/Cu	Evaporate the following: Ni (5000 Å) and Cu (2 μm), on both front and back sides, followed by 325°C, 10 min sintering in forming gas (10% H ₂ and 90% N ₂)
Pd/Ni/Solder	Evaporate the following: Pd (500 Å) and Ni (5,000 Å), on both front and back side, followed by 325°C, 10 min sintering in forming gas (10% H ₂ and 90% N ₂), solder dip
Cr/Pd/Ag	Evaporate the following: Cr (500 Å), Pd (500 Å) and Ag (3 μm), on both front and back side, followed by 400°C, 10 min sintering in N ₂
Thick Film Ag	Screen print back side with silver-aluminum conductor (Thick Film Inc., No. 3398 Ink) and fired at 750°C for 1 min in N ₂ , followed by printing silver conductor (Thick Film Inc., No. 3347 Ink) on front side and sintering at 650°C for 1 min in N ₂

SECTION III

DISCUSSION OF METALLIZATION SYSTEMS

Selection of the metallization systems for this study was determined, for the most part, by consideration of commonly used systems for terrestrial cells. Titanium-palladium-silver is the most familiar metallization system, having been in use for over 20 years, and always used in space cells. Titanium-palladium-silver is also extensively used on terrestrial cells, especially in the earlier designs. Many of the environmental test results found in the cell testing literature is on titanium-palladium-silver. Titanium-silver was a precursor metallization system to titanium-palladium-silver and is also found in the literature on metallization testing. Palladium was added to the titanium-silver system when it was determined that this addition was beneficial against moisture penetration, especially in humidity testing. The test results, herein, verify this fact. Most of the earlier terrestrial solar cells (1978 to 1982), which were purchased under the FSA-JPL Block buy programs (Block I, Block II, Block III, and Block IV), used solder overlay as the main conducting metal. The metallization systems using solder were typically palladium-nickel-solder, gold-nickel-solder, or nickel-solder. The underlying metals were typically plated by palladium, gold, or nickel solutions and then solder dipped. A palladium-nickel-solder system was tested in this program. The palladium and nickel under-layers were vacuum evaporated rather than plated. In fact, all of the metals used in this program were vacuum evaporated excepting the solder dip operations and the thick film silver metallization system.

Solder based metallization systems have been slowly giving way to copper based systems within the last 3 to 4 years in terrestrial metallization systems. Copper has a much higher electrical conductivity than solder, and on a conductivity per pound basis, is much cheaper than solder. Also copper can be ultrasonically bonded to form a superior cell-to-cell interconnection bond compared to soldered interconnections. Westinghouse, for example, uses a copper based metallization system fabricated by first vacuum evaporating titanium and palladium, and then followed by copper plate-up. The cells are interconnected by ultrasonic bonding. Another terrestrial metallization design is plated nickel followed by copper plate-up. Two copper based metallization systems were tested in this program. One system was nickel-copper (both metals were vacuum evaporated); and the other, titanium-palladium-copper (again, all three metals were vacuum evaporated).

One thick film system, a commercial silver paste, was tested in this program. Several solar cell manufacturers (Arco Solar, for example) make cells with thick film silver paste metallization systems and they apply the paste by screen printing, the same as done in this test program.

A chromium-palladium-silver system was tested in this program. This metallization system, to this author's knowledge, is not presently being used on any solar cells being commercially manufactured. However, this system has been used for various lab samples for years. The results show that the chromium-palladium-silver system performs as well or better than the titanium-palladium-silver system after humidity tests.

Table 3-1 presents data on metallization systems used on the FSA Block IV Solar Module procurement (Reference 1).

The Block IV module, built in the 1980 to 1982 time frame, three generations removed from Block I, II, and III, still shows the use of the Ti/Pd/Ag metallization system, as shown in Table 3-1. Most of the contractors were working on more cost effective metallization systems. However, when cell performance was on the line, there was a tendency to fall back on a proven metallization system such as Ti/Pd/Ag, even though more cost-effective systems were being worked on.

Table 3-1. Block IV Metallization Systems

Manufacturer	Metallization System	
	Front Metallization	Back Metallization
Arco Solar	Printed Ag Paste	Printed Al/Printed Ag Paste
Applied Solar Energy Corporation (ASEC)	Vacuum Evaporated Ti/Pd/Ag	Vacuum Evaporated Ti/Pd/Ag
General Electric (GE)	Printed Ag Paste	Printed Al/Printed Ag Paste
Motorola	Plated Pd/Ni/Solder Dip	Plated Pd/Ni/Solder Dip
Photowatt	Plated Ni/Solder Dip	Plated Ni/Solder Dip
Solarex	Vacuum Evaporated Ti/Pd/Ag	Vacuum Evaporated Ti/Pd/Ag
Spire	Vacuum Evaporated Ti/Pd/Ag	Vacuum Evaporated Ti/Pd/Ag

SECTION IV
TEST EQUIPMENT

Figure 4-1 is a picture of the humidity chamber used for humidity exposure in this test program. The chamber was manufactured by Blue M Electric Company, Blue Island, Illinois, and is Model No. AC-7502HA-TDA-1(Y). The chamber was developed for long term high temperature/humidity testing that is capable of meeting steady-state requirements such as found in Mil-Std-202C, Method 106B, "continuous operation for 56 days, with low water consumption (less than 1 gallon/24 hours)." Temperature range is 12°C above ambient to +93°C ($\pm 1/2^\circ\text{C}$). The relative humidity range is from 40% to 98% saturation.

Figure 4-2 is a picture of the temperature cycling chamber used for temperature cycling in this test program. The chamber was manufactured by Blue M Electric Company, Blue Island, Illinois, and is Model No. LN-270B-1MP, temperature range -200°C to +300°C. The chamber has a 3kW heater for above ambient heating and is fitted for liquid nitrogen for below ambient cooling. The unit is microprocessor controlled and can be programmed to run various temperature cycling programs.

Figures 4-3 and 4-4 are pictures of the current/voltage (I-V) test equipment. In Figure 4-3, the light source (Solar Simulator, Model No. XT-10) was manufactured by Spectrolab, Sylmar, California. The cell holder equipment beneath the light source is water cooled and set to maintain the cell sample at 28°C. The I-V Plotter and computer equipment are shown in Figure 4-4. The I-V Plotter was manufactured by Tektronix Inc., Model No. 4662. The computer equipment was manufactured by Tektronix Inc., Model No. 4052.

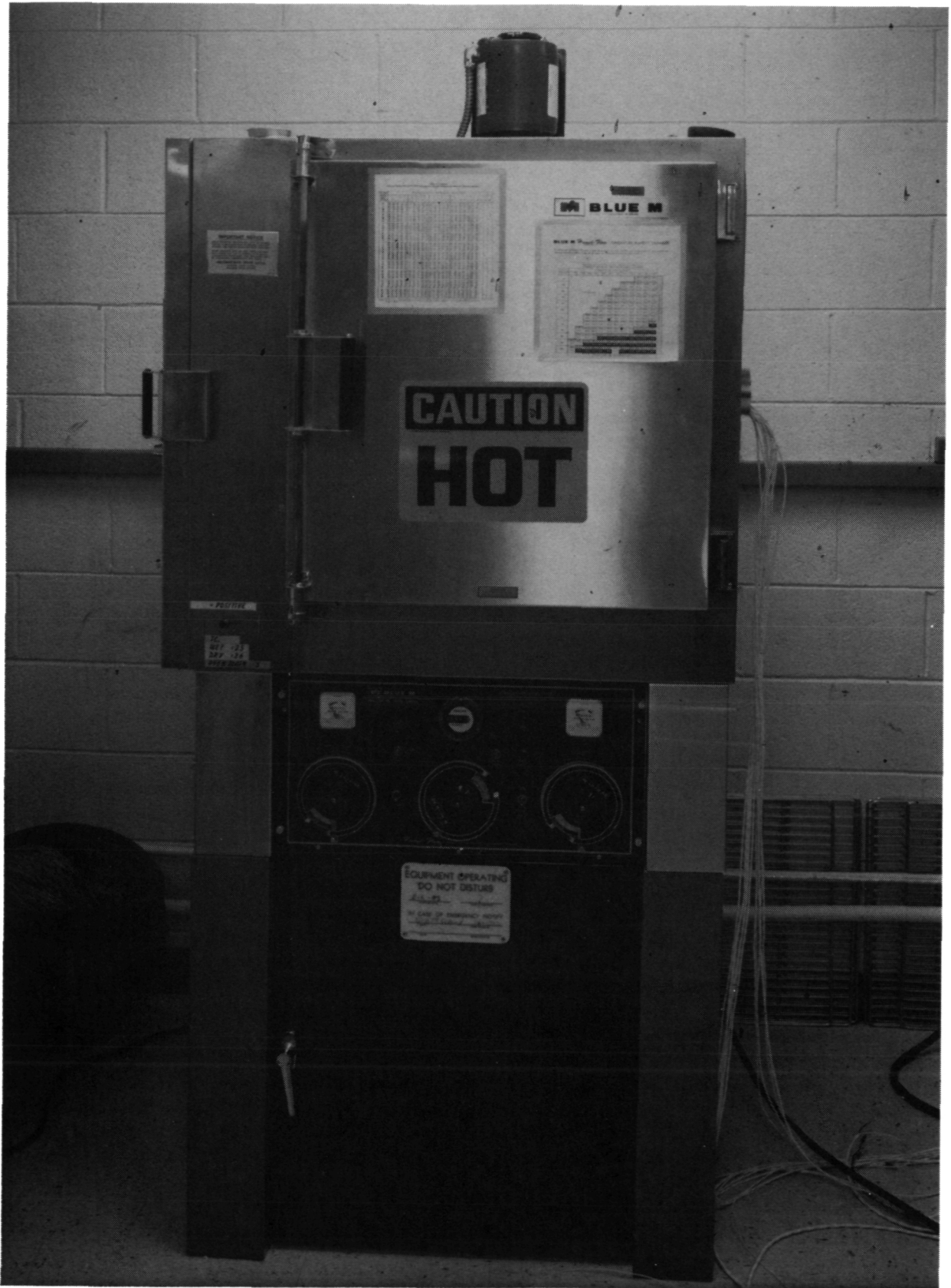


Figure 4-1. Temperature and Humidity Chamber

ORIGINAL PAGE IS
OF POOR QUALITY

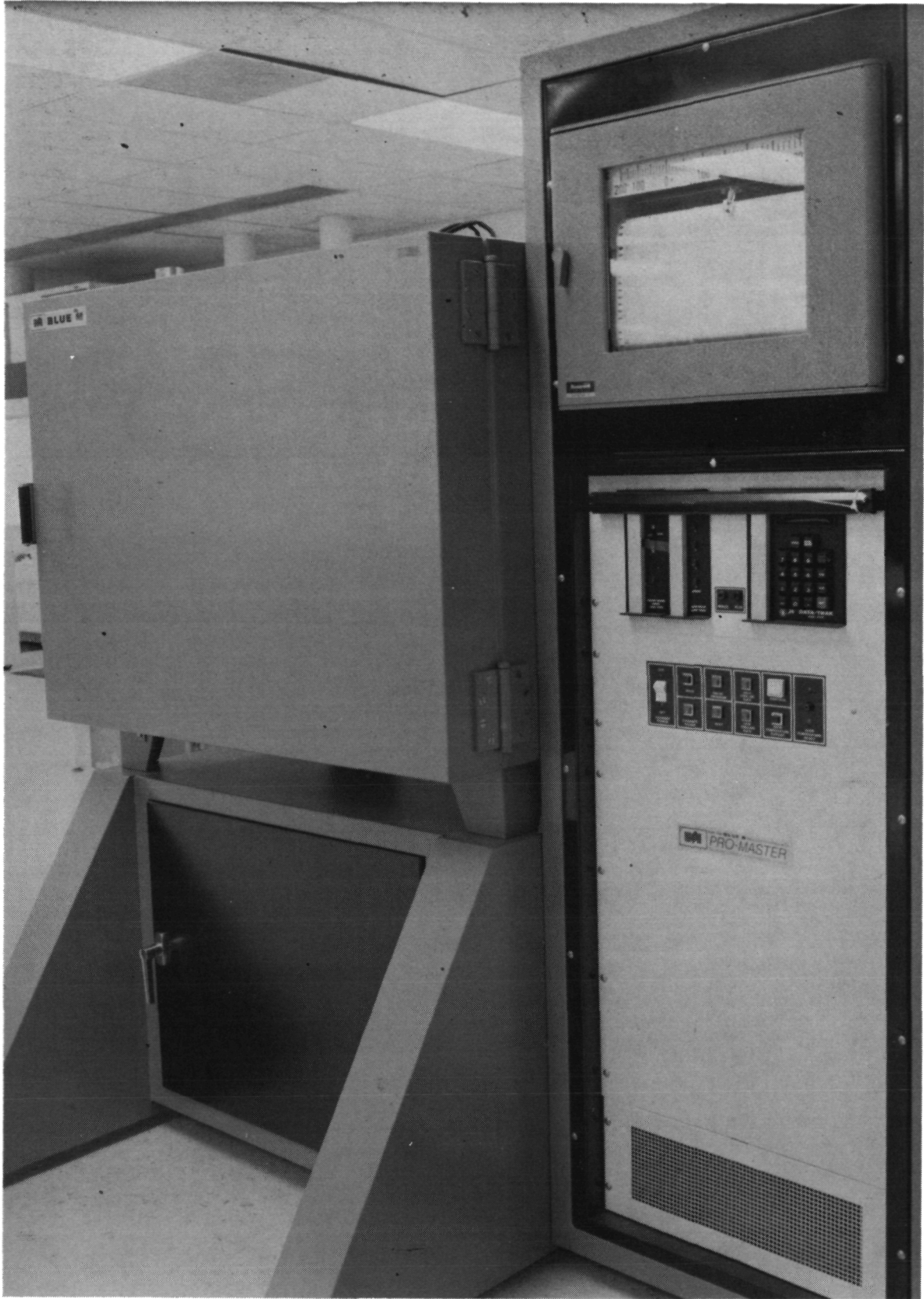


Figure 4-2. Temperature Cycling Chamber

UNCLASSIFIED
DATE 03-01-2011 BY 60322 UCBAW

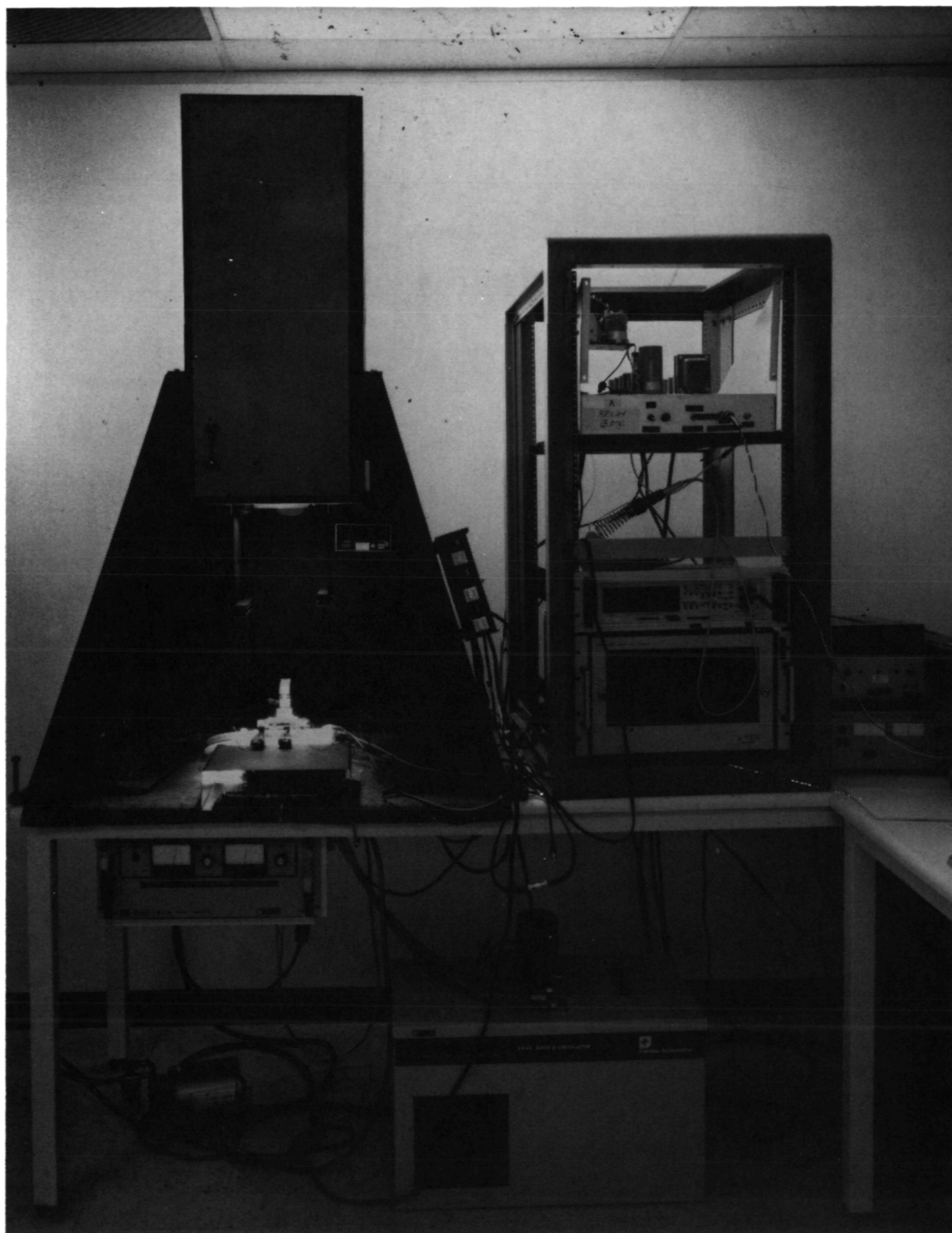


Figure 4-3. I-V Test Equipment, Light Source

ORIGINAL PAGE IS
OF POOR QUALITY

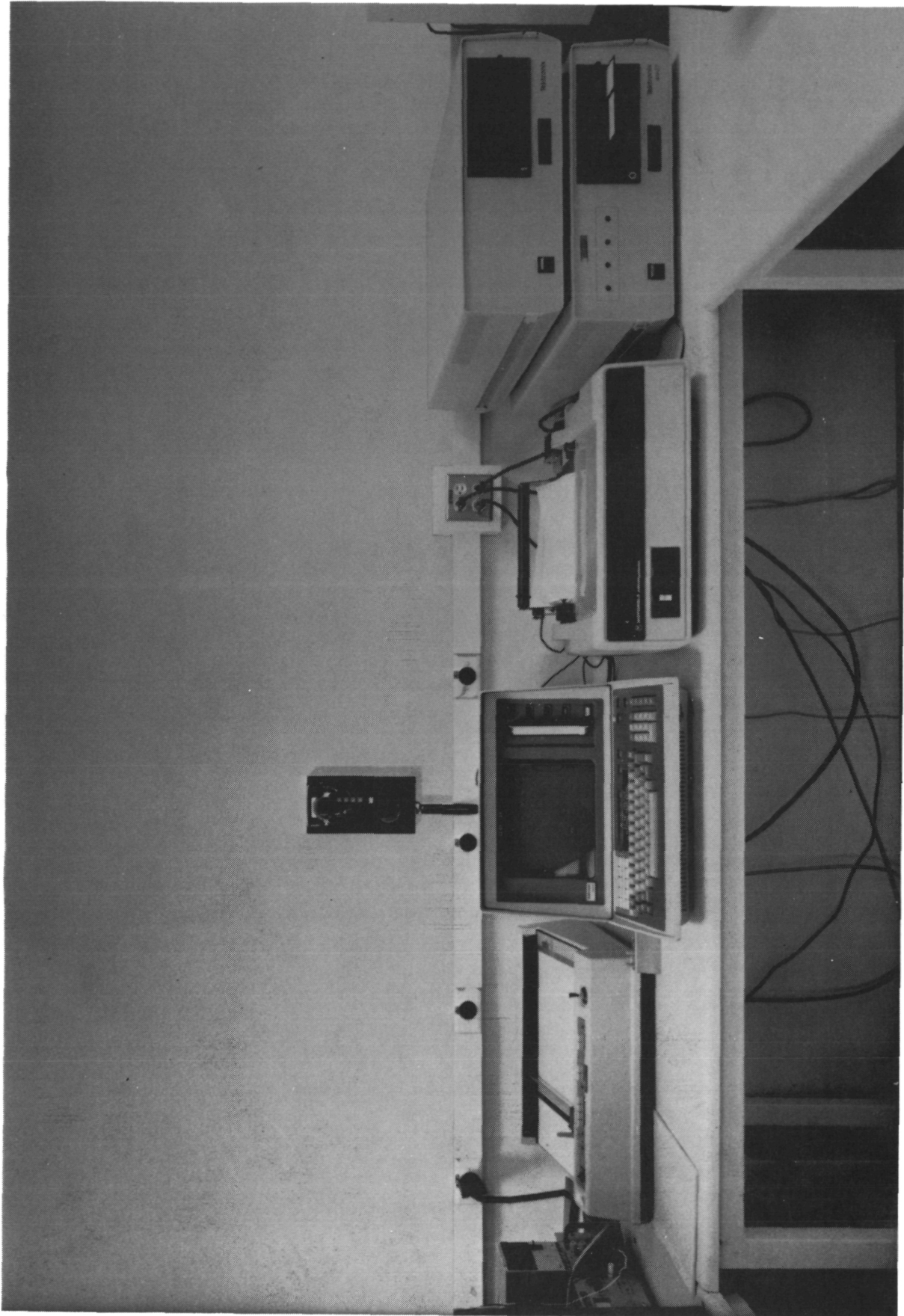


Figure 4-4. I-V Test Equipment, Data Printout

SECTION V
TEST PROGRAM

Approximately 129 cells were used in the test program. Seven sets of six cells each (43 total) of seven different metallization systems were subjected to temperature cycling tests. Similarly, seven sets of six cells each (43 total) of the seven different metallization systems were subjected to humidity tests. Seven sets of six cells each (43 total) of the seven different metallization systems were used as controls. Tables 5-1 and 5-2 outline the temperature cycling and humidity tests.

Table 5-1. Temperature Cycling Tests^{a,b}

No. of Cells, No. of Cell Types	I-V Test	No. of Temp Cycles	I-V Test	No. of Temp Cycles	I-V Test	No. of Temp Cycles	I-V Test	No. of Temp Cycles	I-V Test	No. of Temp Cycles	I-V Test
6 cells ea of 7 metal types, 43 cells total	43 total	10 cycles	43 total	30 cycles (40 cycles total)	43 total	100 cycles (140 cycles total)	43 total	300 cycles (440 cycles total)	43 total	560 cycles (1,000 cycles total)	43 total
											6 ea x 7 sets

^aTemperature Excursions were:
From -65°C for approximately 6 min dwell at -65°C to +150°C for approximately 6 min dwell at 150°C.
Approximately 14 min ramp time between temperatures. Total cycle time was approximately 40 min/cycle.

^bCell Metal Types: B1 - Ti/Ag B3 - Ti/Pd/Cu B5 - Pd/Ni/Solder B7 - Thick Film Ag Paste
B2 - Ti/Pd/Ag B4 - Ni/Cu B6 - Cr/Pd/Ag

Table 5-2. Humidity Exposure Tests^{a,b}

No. of Cells, No. of Cell Types	I-V Test	Humidity (No. Days Exposure)	I-V Test	Humidity (No. Days Exposure)	I-V Test	Humidity (No. Days Exposure)	I-V Test	Humidity (No. Days Exposure)	I-V Test	Humidity (No. Days Exposure)	I-V Test
6 cells ea of 7 metal type (43 cells total)	43 total	3 days	43 total	10 days (13 days total)	43 total	20 days (33 days total)	43 total	30 days (63 days total)	43 total	60 days (123 days total)	43 total
											6 ea x 7 sets

^aHumidity conditions were 60°C at 100% saturation for the 3-days and 10 days exposures. Conditions were 70°C at 98% relative humidity for the 20, 30 and 60-day exposures. Differences in humidity conditions were due to testing piggyback with other items which had priority on humidity conditions.

^bCell Metal Types: B1 - Ti/Ag B3 - Ti/Pd/Cu B5 - Pd/Ni/Solder B7 - Thick Film Ag Paste
B2 - Ti/Pd/Ag B4 - Ni/Cu B6 - Cr/Pd/Ag

SECTION VI

TEST RESULTS

A. I-V CHARACTERISTICS AFTER ENVIRONMENTAL EXPOSURE

Solar cells from each of the seven metallization systems were tested for I-V characteristics after each environmental exposure (see the description of the Test Program). Nine parameters were measured on each I-V test which included: short circuit current, mA (I_{sc}); open circuit voltage, mV (V_{oc}); maximum power, mW (P_{mp}); current at maximum power, mA (I_{mp}); voltage at maximum power, mV (V_{mp}); cell efficiency (η); fill factor (FF); cell series resistance, ohms (R_s); and cell shunt resistance, ohms (R_{sh}).^{*} A very condensed summary of results is shown in Table 6-1. Extensive light I-V test data are tabulated and presented in the Appendix.

I-V data for each of the seven metallization cell types were generated. The data include: efficiency and fill factor versus temperature cycling; and efficiency and series resistance versus number of days of humidity exposure. The I-V curves are presented in the figures herein.

Pictures at 40 times magnification were taken of selected cell specimens before and after testing. The pictures are presented in the figures herein.

^{*}The shunt resistance values in this work are to be taken as a range or trend as opposed to the absolute values. This is because the algorithms used in the computer program to calculate shunt resistance values, although measured in accordance with one of the ASTM standards, tends to generate numbers that are overly responsive to normal test variations.

Table 6-1. Summary of the Results for Temperature and Humidity Exposure Tests

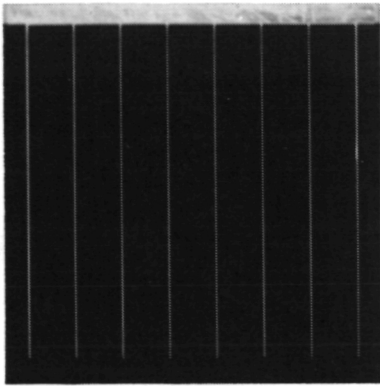
Metal System (2x2 cm Cells)	% Change in Cell Efficiency After 1,000 Temperature Cycles ^{1,2}	Ranking (Least Degradation)	% Change in Cell Efficiency After 123 Days Humidity Exposure ^{2,3}	Ranking (Least Degradation)
Ti/Ag	-4.19	2	-30.15	4
Ti/Pd/Ag	-3.69	1	-11.35	2
Pd/Ni/Cu	-20.7	7	-54.43	6
Ni/Cu	-17.10	6	-71.14	7
Pd/Ni/Solder	-6.99	4	-12.97	3
Cr/Pd/Ag	-4.6	3	-9.33	1
Thick Film Ag	-14.32	5	-44.40	5

¹Temperature excursions were: from -65°C for approximately 6 min dwell at -65°C to +150°C for approximately 6-min dwell at 150°C. Approximately 14 min ramp time between temperatures. Total cycle time was approximately 40 min/cycle.

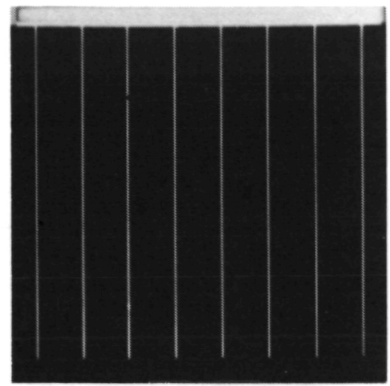
²Humidity conditions were: 60°C at 100% saturation for first 13 days and 70°C at 98% relative humidity for 14 through 123 days.

³I-V test conditions for all tests were: AM1 at 28°C.

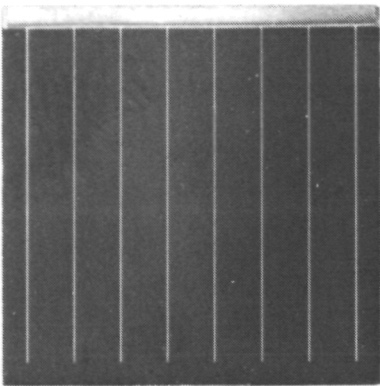
ORIGINAL PAGE IS
OF POOR QUALITY



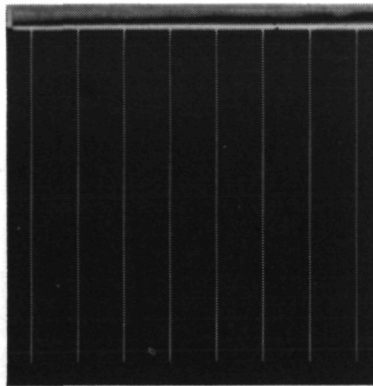
(a) Ti/Ag



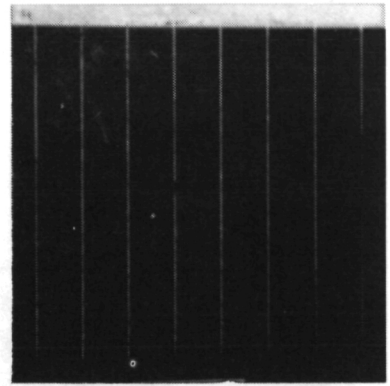
(b) Ti/Pd/Ag



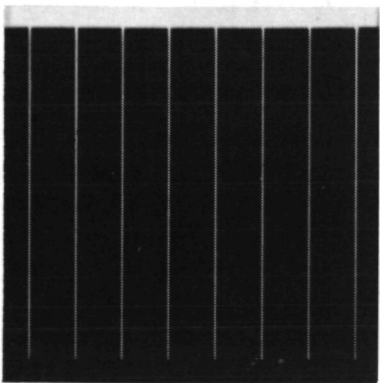
(c) Ti/Pd/Cu



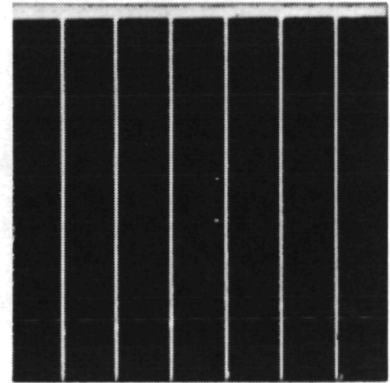
(d) Ni/Cu



(e) Pd/Ni/SOLDER



(f) Cr/Pd/Ag

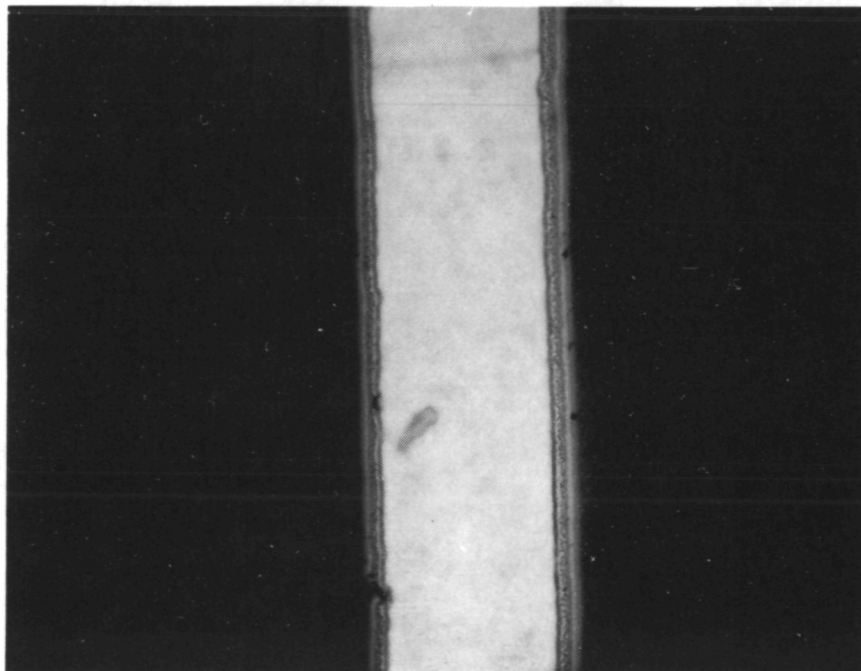


(g) THICK FILM Ag PASTE

Figure 6-1. Control Cells (No Environmental Exposures) for Ti/Ag, Ti/Pd/Ag, Ti/Pd/Cu, Ni/Cu, Pd/Ni/Solder, Cr/Pd/Ag, and Thick Film Ag Paste

Figure 6-2 shows a grid line on each of three cells of the Ti/Ag metallization system as follows:

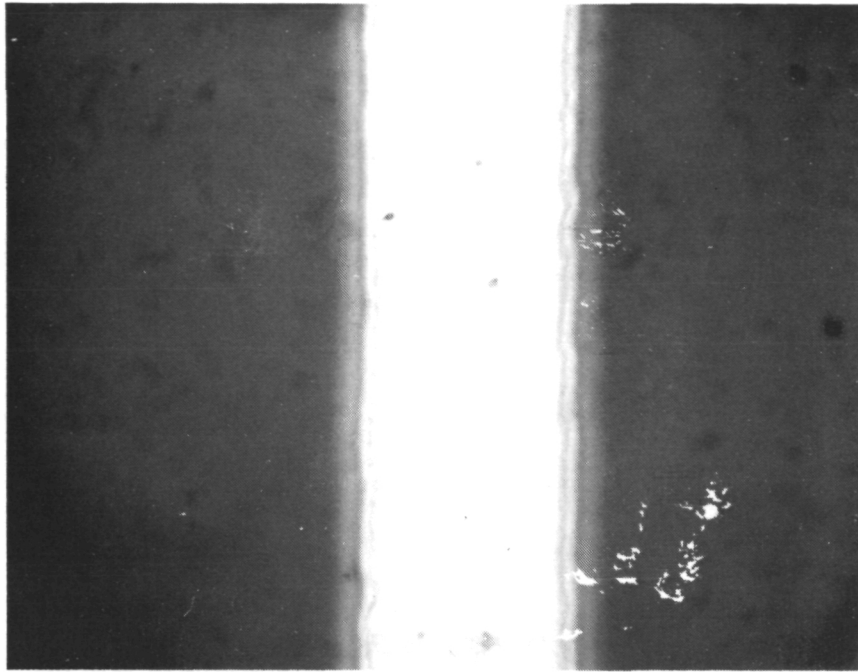
- (a) Cell 19, control cell, 40x magnification.
- (b) Cell 34, after 1000 temperature cycles (-65°C to 150°C), 40x magnification.
- (c) Cell 18, after 123 days humidity exposure (70°C at 98% relative humidity), 16x magnification.



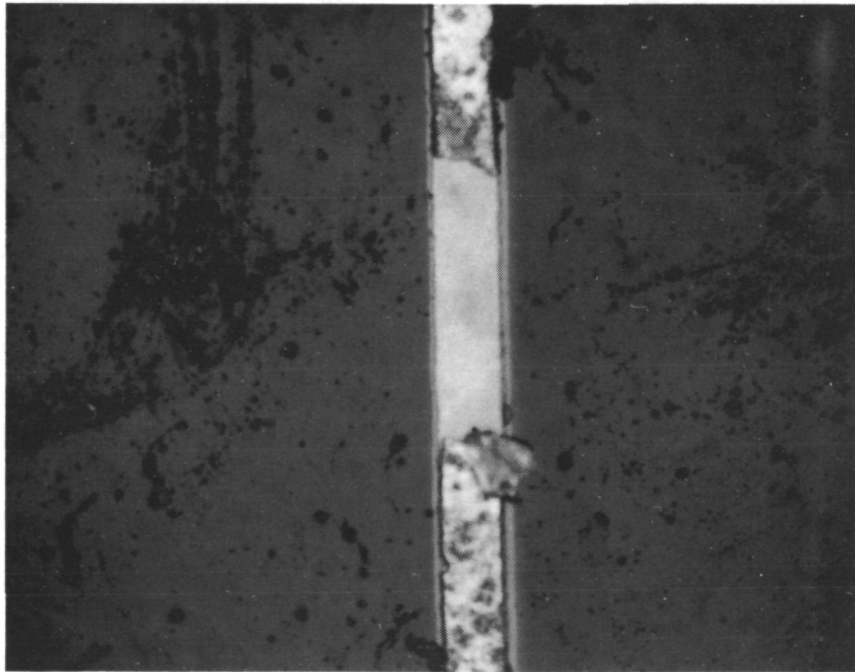
(a) Control Cell

Figure 6-2. Control Cells, After Temperature Cycling, and After Humidity Exposure, Ti/Ag (a, b and c)

ORIGINAL PAGE IS
OF POOR QUALITY



(b) After 1000 Temperature Cycles

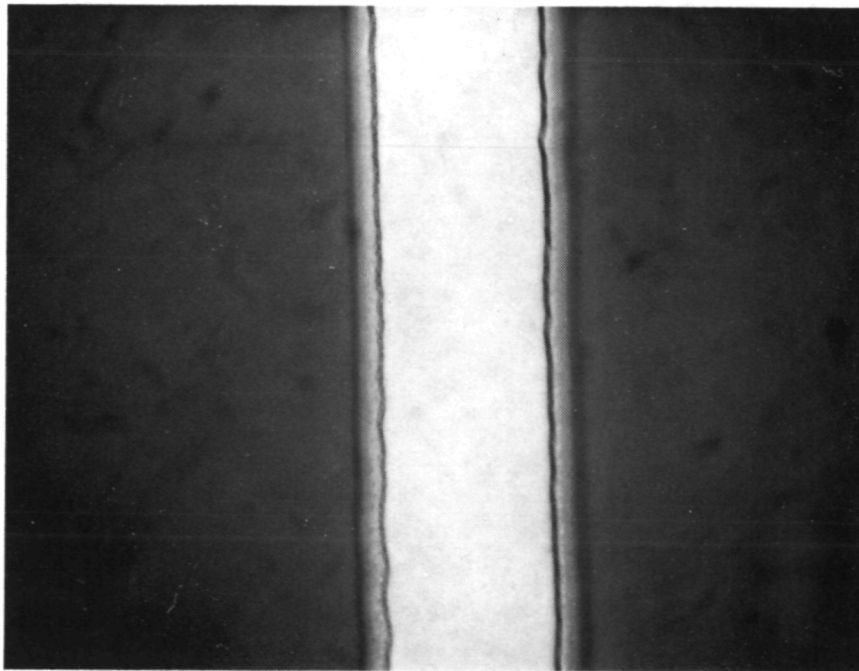


(c) After 123 Days Humidity Exposure

Figure 6-2. (Cont'd)

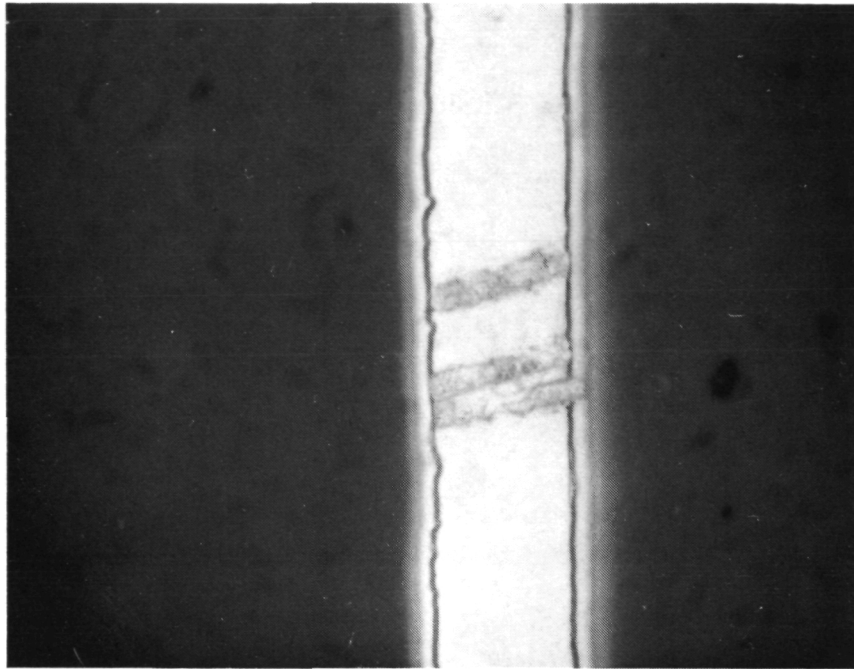
Figure 6-3 shows a grid line on each of the three cells of the Ti/Pd/Ag metallization system as follows:

- (a) Cell 42, control cell, 40x magnification.
- (b) Cell 37, after 1000 temperature cycles (-65°C to 150°C), 40x magnification.
- (c) Cell 19, after 123 days humidity exposure (70°C at 98% relative humidity), 40x magnification.

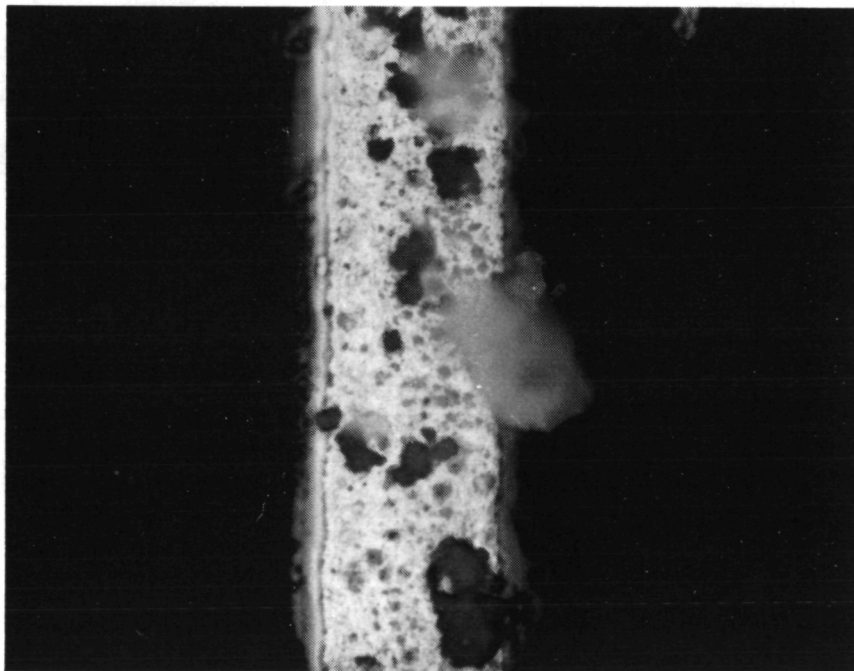


(a) Control Cell

Figure 6-3. Control Cells, 40x, After Temperature Cycling, and After Humidity Exposure, Ti/Pd/Ag (a, b and c)



(b) After 1000 Temperature Cycles

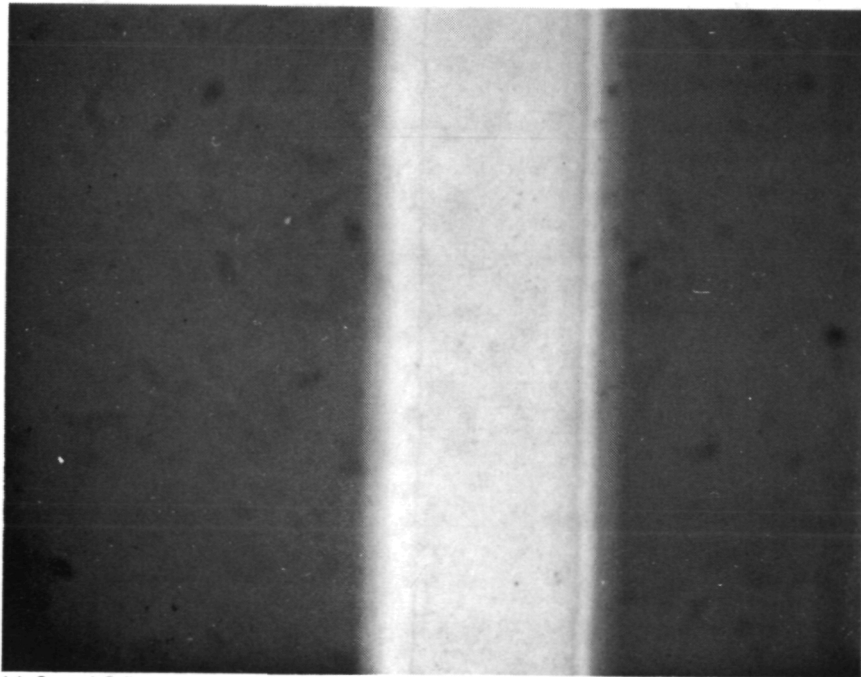


(c) After 123 Days Humidity Exposure

Figure 6-3. (Cont'd)

Figure 6-4 shows a grid line on each of the three cells of the Ti/Pd/Cu metallization system as follows:

- (a) Cell 25, control cell, 40x magnification.
- (b) Cell 45, after 1000 temperature cycles (-65°C to 150°C), 40x magnification.
- (c) Cell 28, after 123 days humidity exposure (70°C to 98% relative humidity), 40x magnification.



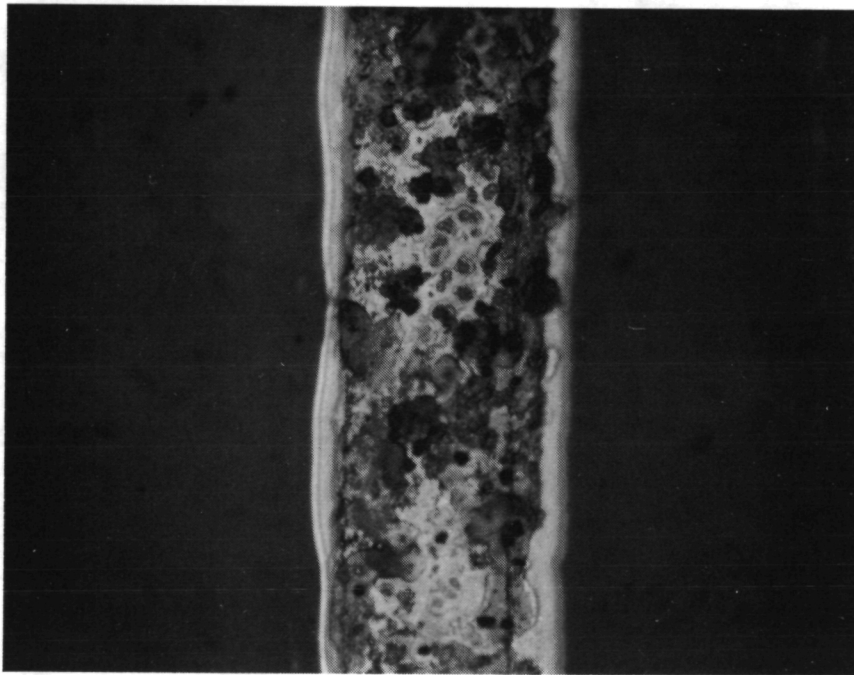
(a) Control Cell

Figure 6-4. Control Cells, 40x, After Temperature Cycling, and After Humidity Exposure, Ti/Pd/Cu (a, b and c)

ORIGINAL PAGE IS
OF POOR QUALITY



(b) After 1000 Temperature Cycles

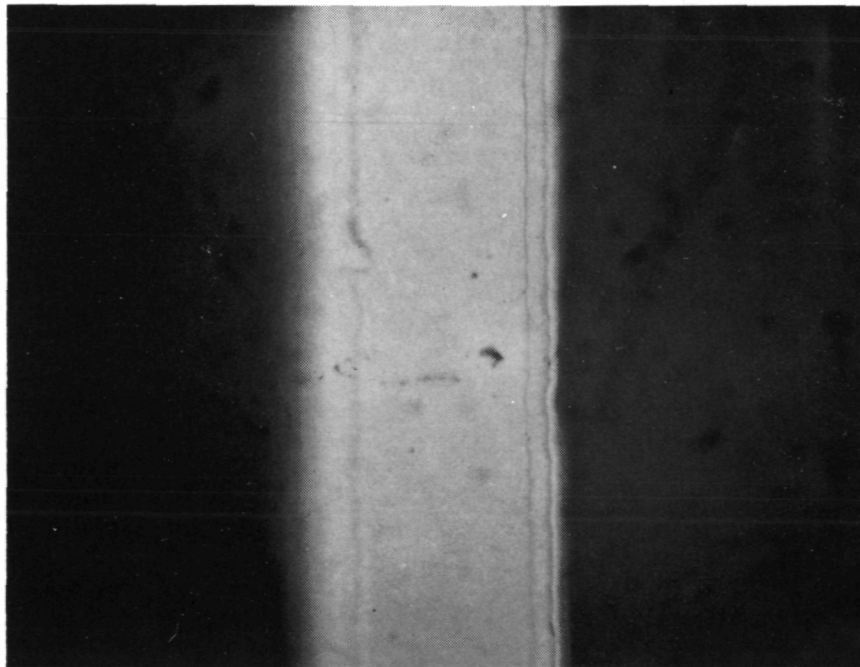


(c) After 123 Days Humidity Exposure

Figure 6-4. (Cont'd)

Figure 6-5 shows a grid line on each of the three cells of the Ni/Cu metallization system as follows:

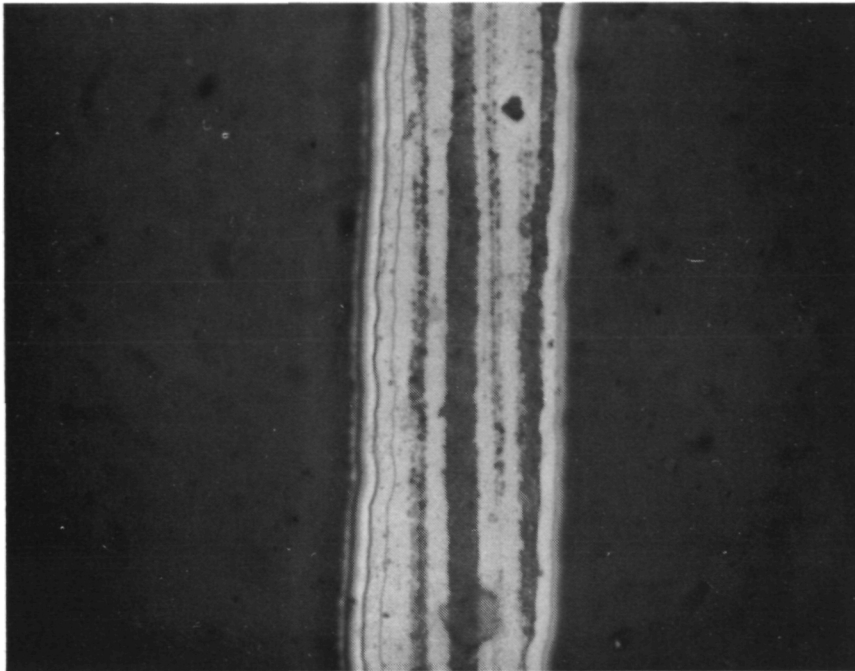
- (a) Cell 30, control cell, 40x magnification.
- (b) Cell 30, after 1000 temperature cycles (-65°C to 150°C), 40x magnification.
- (c) Cell 37, after 123 days humidity exposure (70°C at 98% relative humidity), 40x magnification.



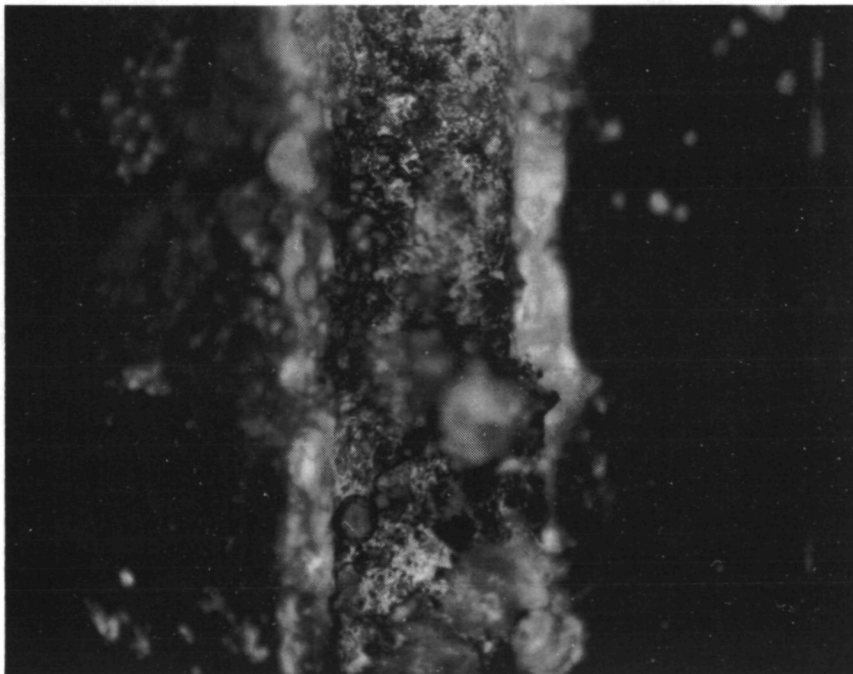
(a) Control Cell

Figure 6-5. Control Cells, 40x, After Temperature Cycling, and After Humidity Exposure, Ni/Cu (a, b and c)

ORIGINAL PAGE IS
OF POOR QUALITY



(b) After 1000 Temperature Cycles

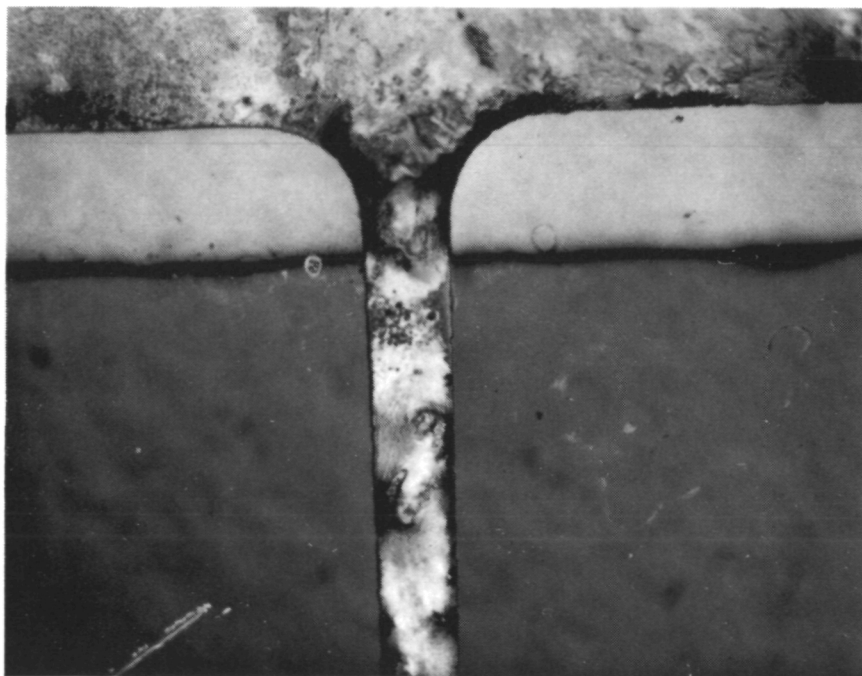


(c) After 123 Days Humidity Exposure

Figure 6-5. (Cont'd)

Figure 6-6 shows a grid line on each of the three cells of the Pd/Ni/Solder metallization system as follows:

- (a) Cell 22, control cell, 16x magnification.
- (b) Cell 30, after 1000 temperature cycles (-65°C to 150°C), 16x magnification.
- (c) Cell 24, after 123 days humidity exposure (70°C at 98% relative humidity), 16x magnification.



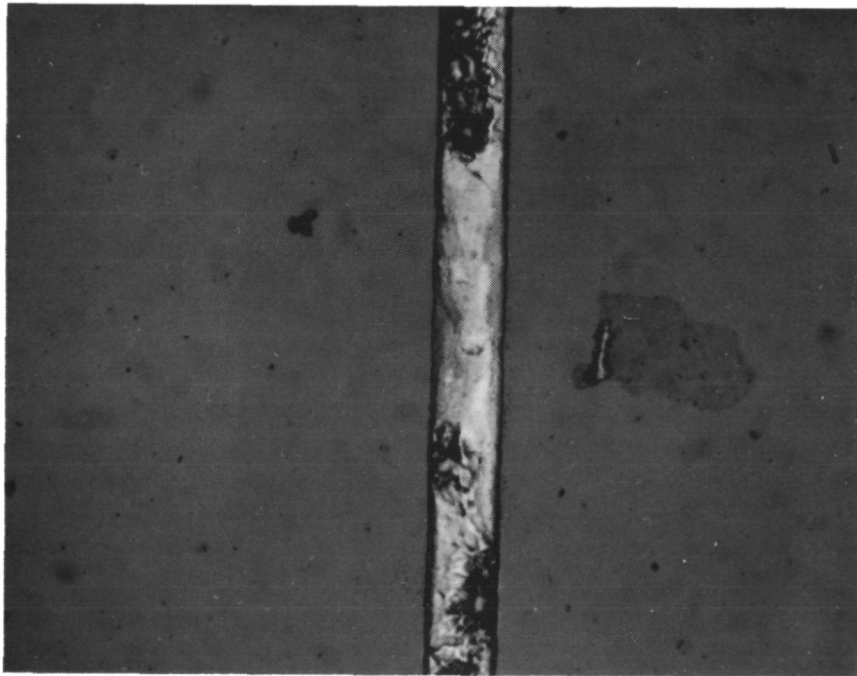
(a) Control Cell

Figure 6-6. Control Cells, 16x, After Temperature Cycling, and After Humidity Exposure, Pd/Ni/Solder (a, b and c)

ORIGINAL PAGE IS
OF POOR QUALITY



(b) After 1000 Temperature Cycles

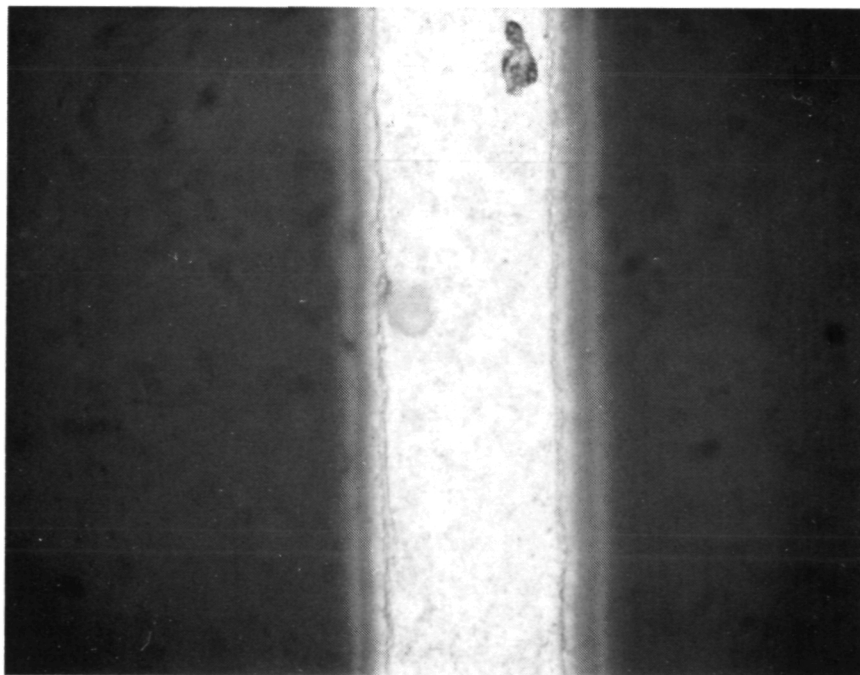


(c) After 123 Days Humidity Exposure

Figure 6-6. (Cont'd)

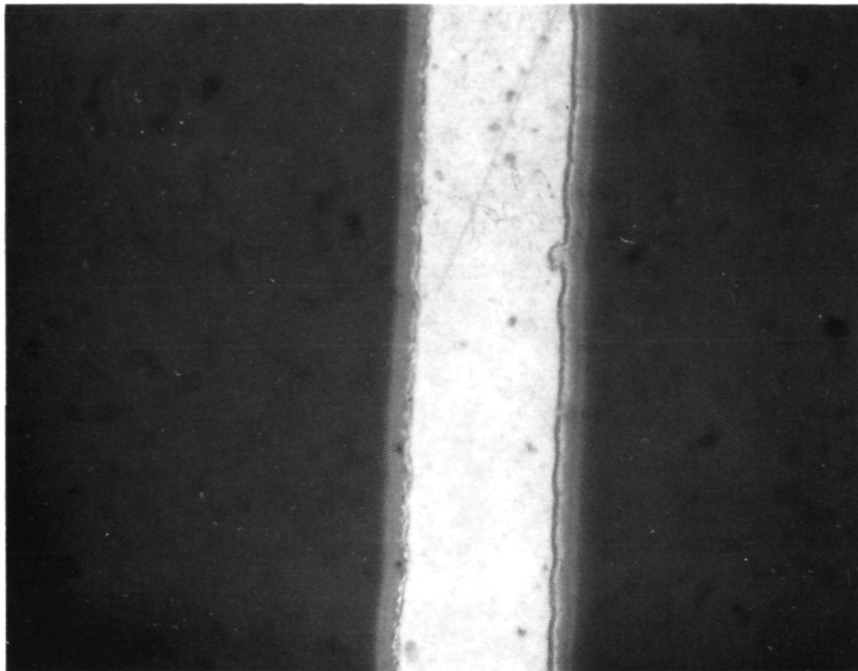
Figure 6-7 shows a grid line on each of the three cells of the Cr/Pd/Ag metallization system as follows:

- (a) Cell 26, control cell, 40x magnification.
- (b) Cell 21, after 1000 temperature cycles (-65°C to 150°C), 40x magnification.
- (c) Cell 29, after 123 days humidity exposure (70°C at 98% relative humidity), 40x magnification.

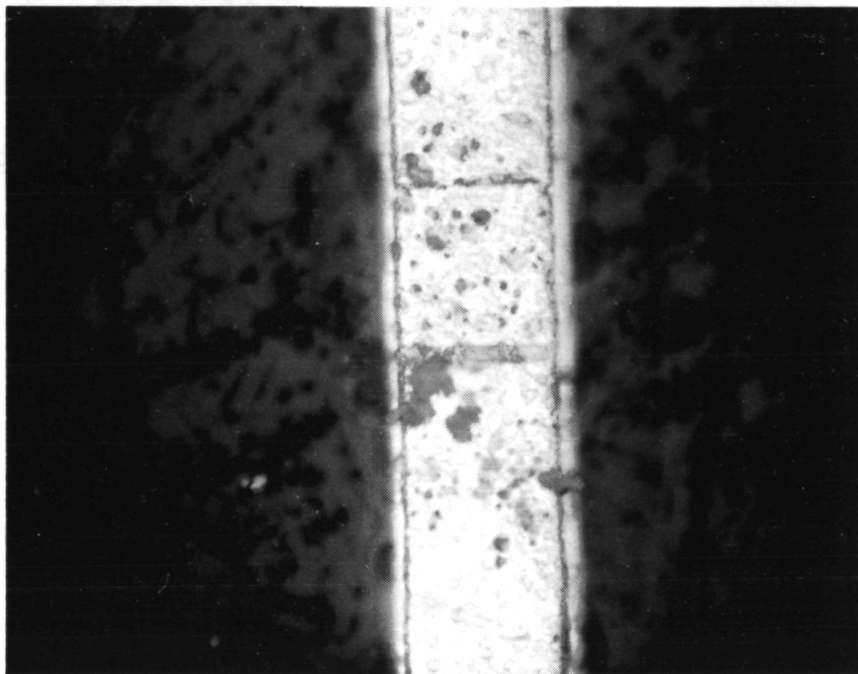


(a) Control Cell

Figure 6-7. Control Cells, 40x, After Temperature Cycling, and After Humidity Exposure, Cr/Pd/Ag (a, b and c)



(b) After 1000 Temperature Cycles

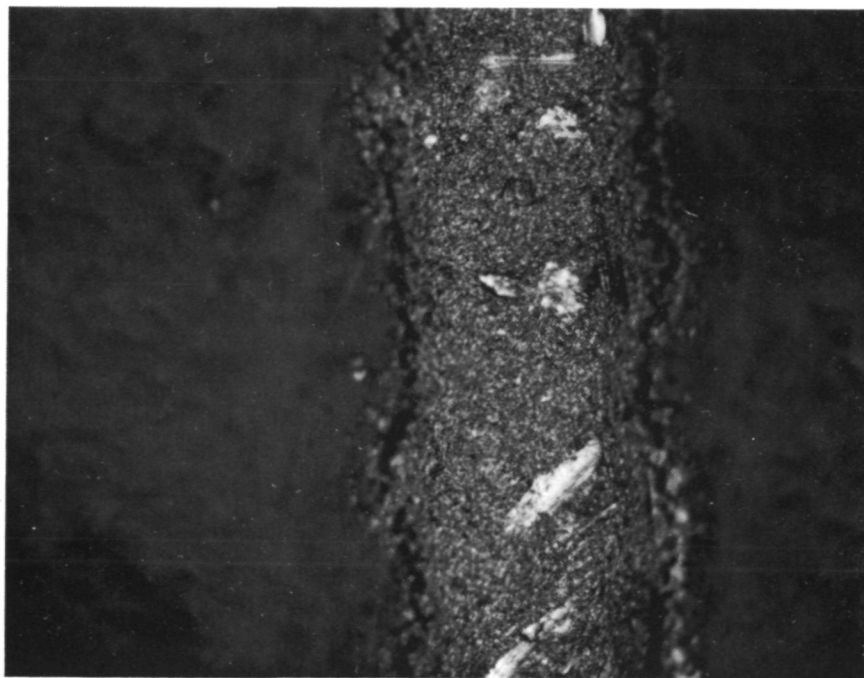


(c) After 123 Days Humidity Exposure

Figure 6-7. (Cont'd)

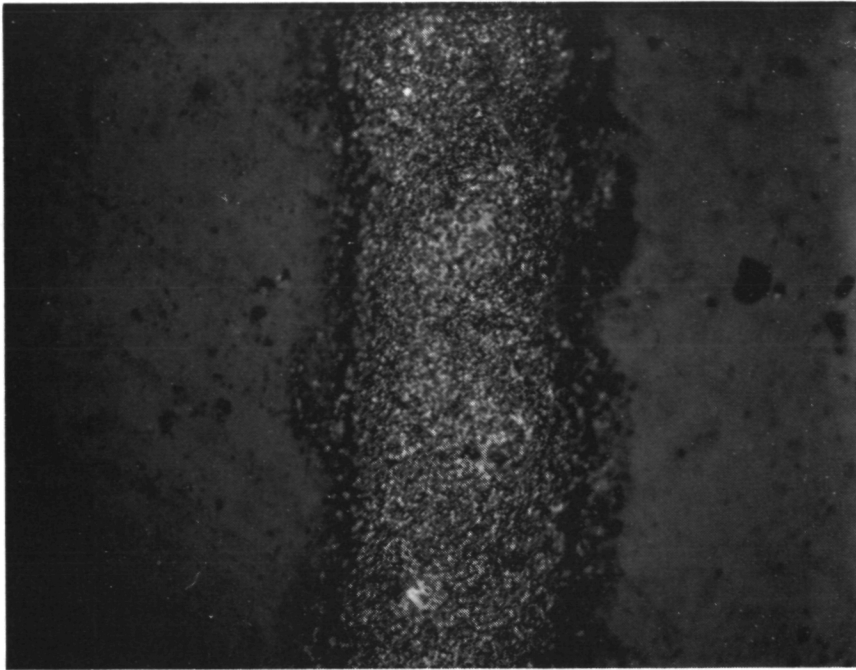
Figure 6-8 shows a grid line on each of the three cells of the Thick Film Ag Paste metallization system as follows:

- (a) Cell 24, control cell, 40x magnification.
- (b) Cell 44, after 1000 temperature cycles (-65°C to 150°C), 40x magnification.
- (c) Cell 61, after 123 days humidity exposure (70°C at 98% relative humidity), 40x magnification.

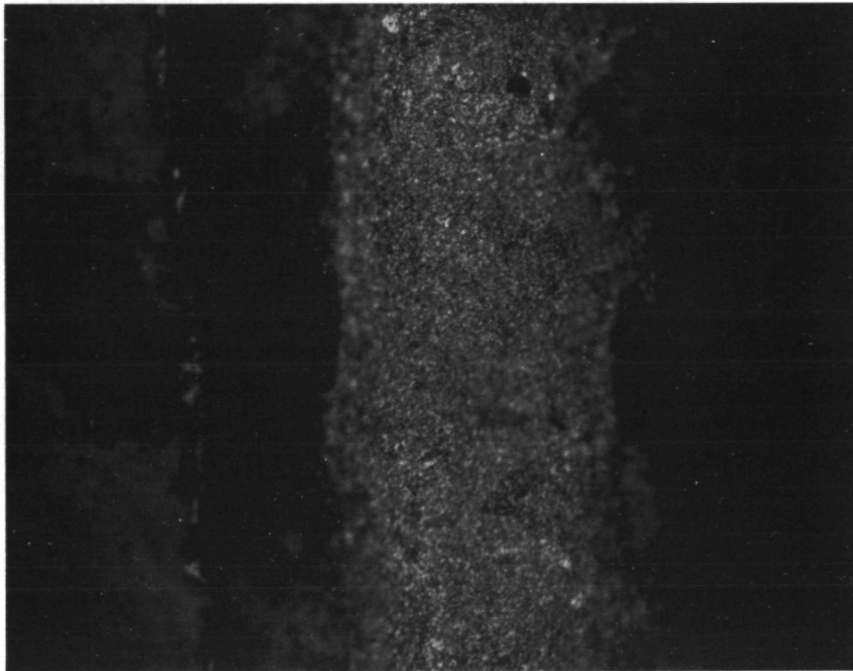


(a) Control Cell

Figure 6-8. Control Cells, 40x, After Temperature Cycling, and After Humidity Exposure, Thick Film Ag Paste (a, b and c)



(b) After 1000 Temperature Cycles



(c) After 123 Days Humidity Exposure

Figure 6-8. (Cont'd)

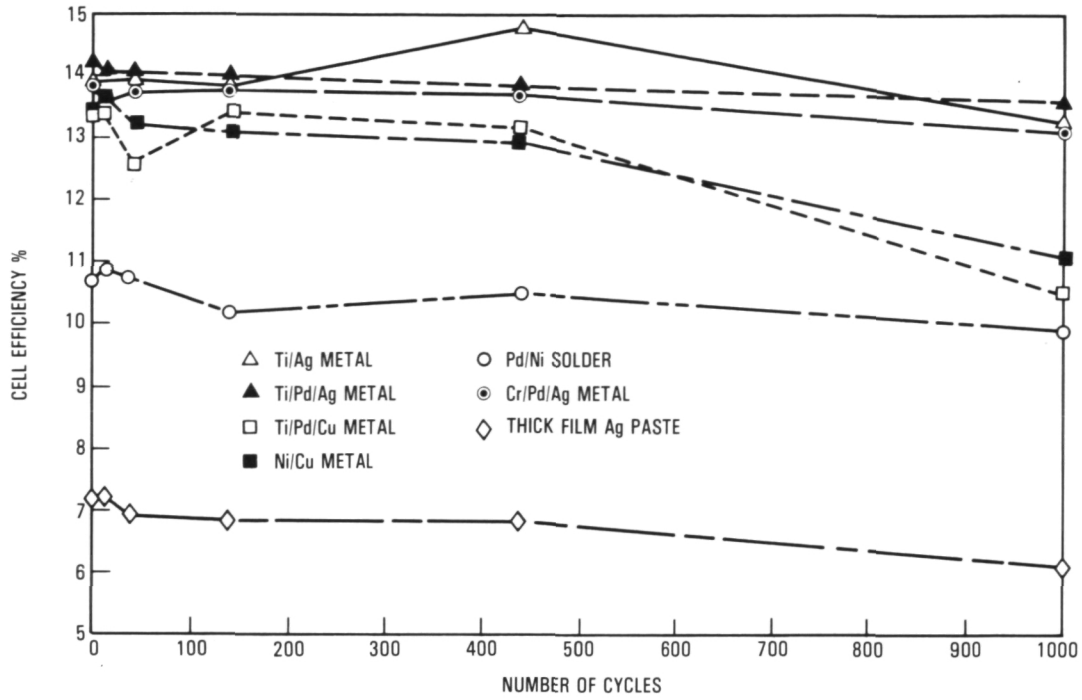


Figure 6-9. Temperature Cycling: Efficiency Versus Number of Cycles for Seven Metallization Systems

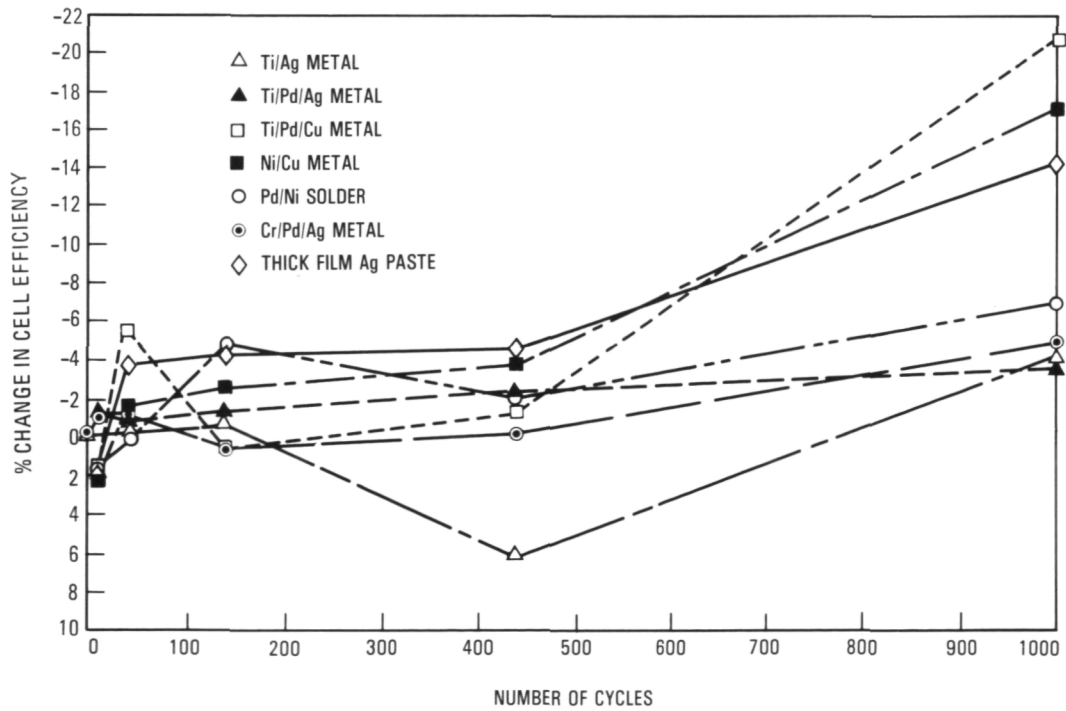


Figure 6-10. Temperature Cycling: Percent Change in Efficiency Versus Number of Cycles for Seven Metallization Systems

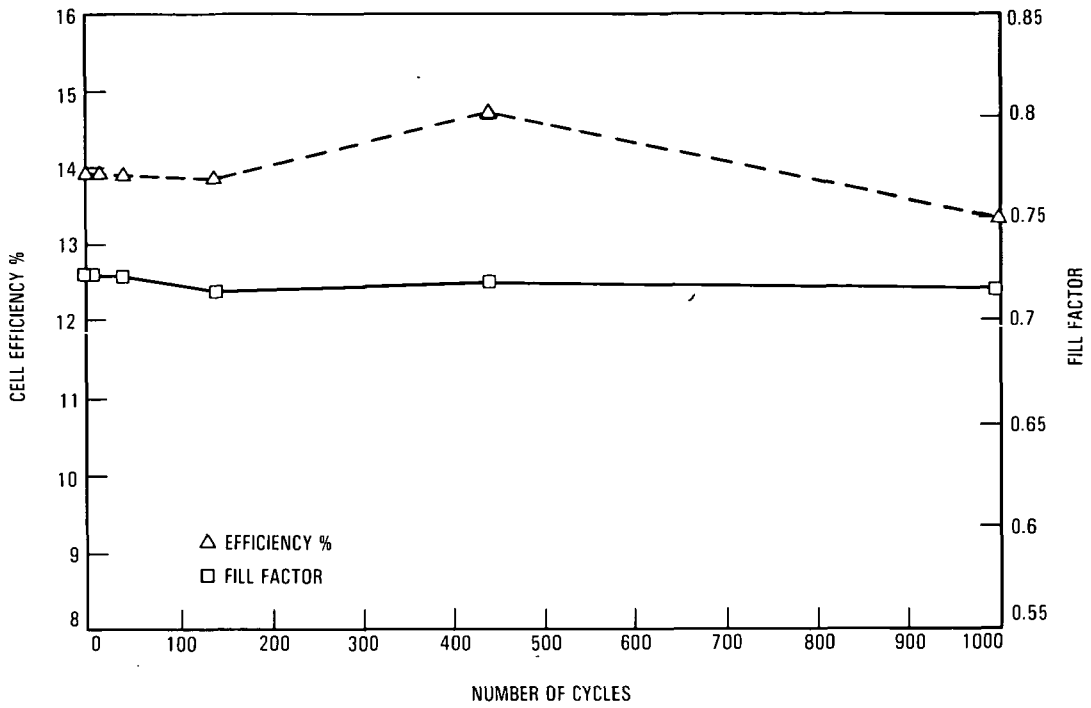


Figure 6-11. Temperature Cycling: Efficiency and Fill Factor Versus Number of Cycles, Ti/Ag

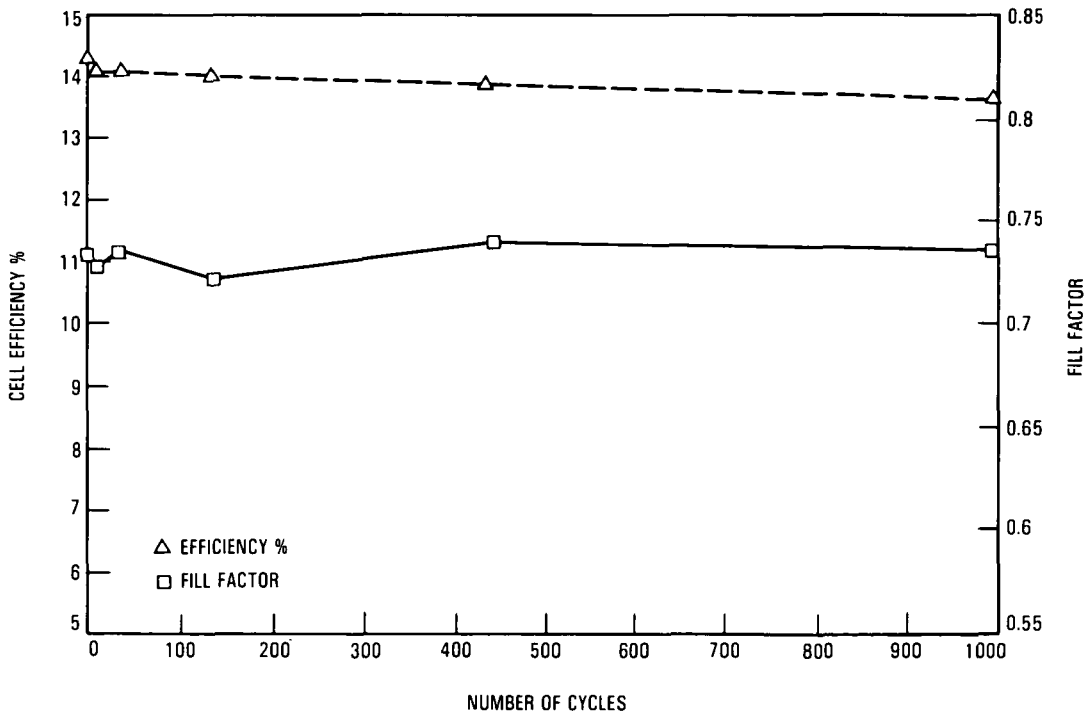


Figure 6-12. Temperature Cycling: Efficiency and Fill Factor Versus Number of Cycles, Ti/Pd/Ag

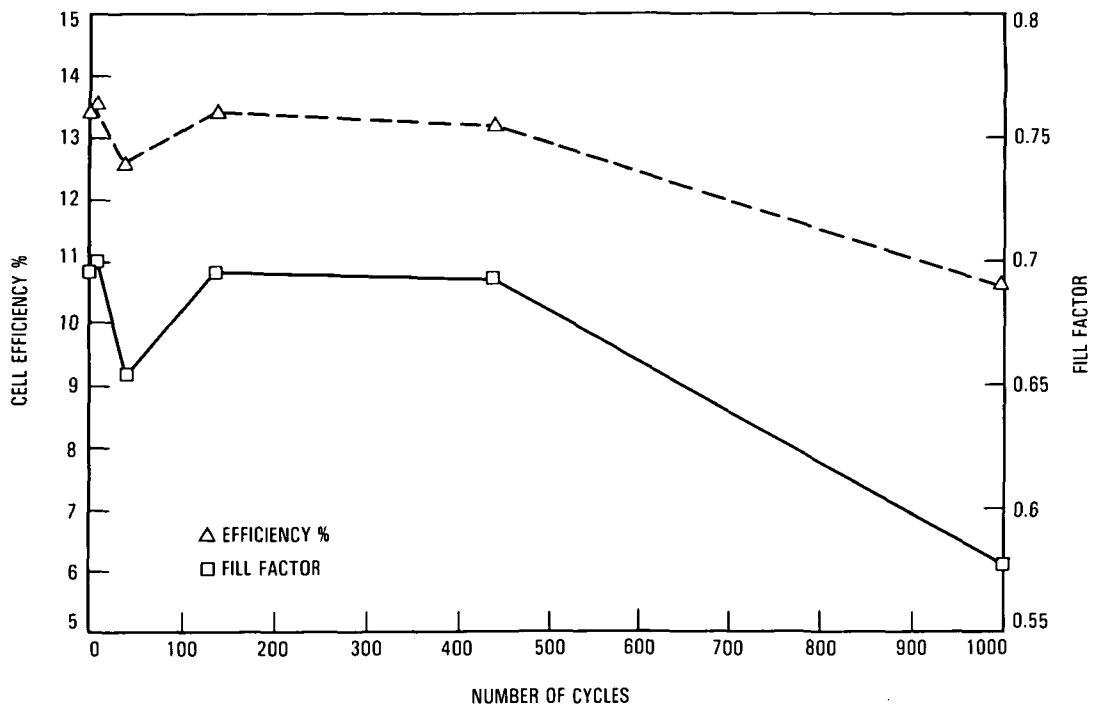


Figure 6-13. Temperature Cycling: Efficiency and Fill Factor Versus Number of Cycles, Ti/Pd/Cu

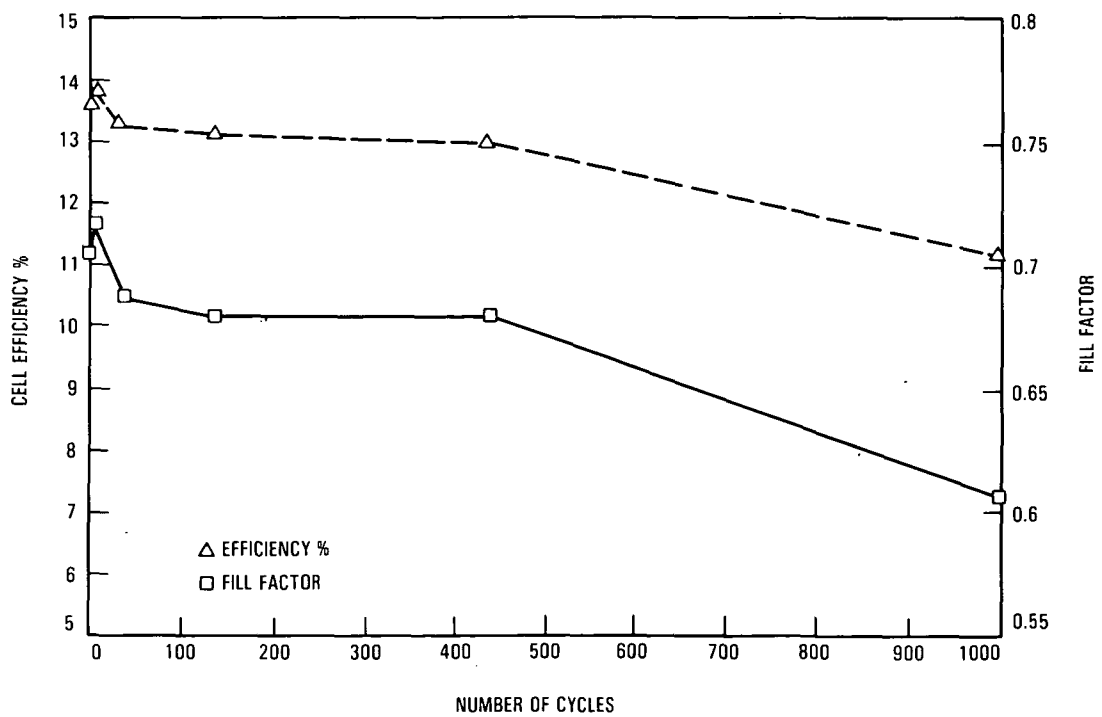


Figure 6-14. Temperature Cycling: Efficiency and Fill Factor Versus Number of Cycles, Ni/Cu

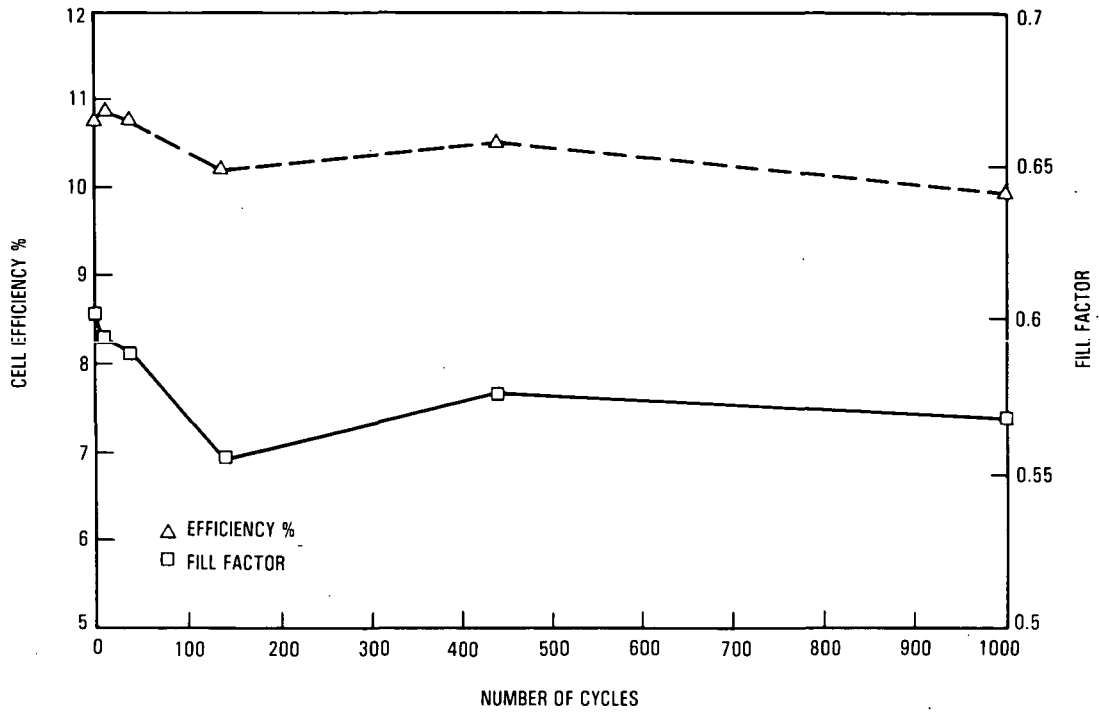


Figure 6-15. Temperature Cycling: Efficiency and Fill Factor Versus Number of Cycles, Pd/Ni/Solder

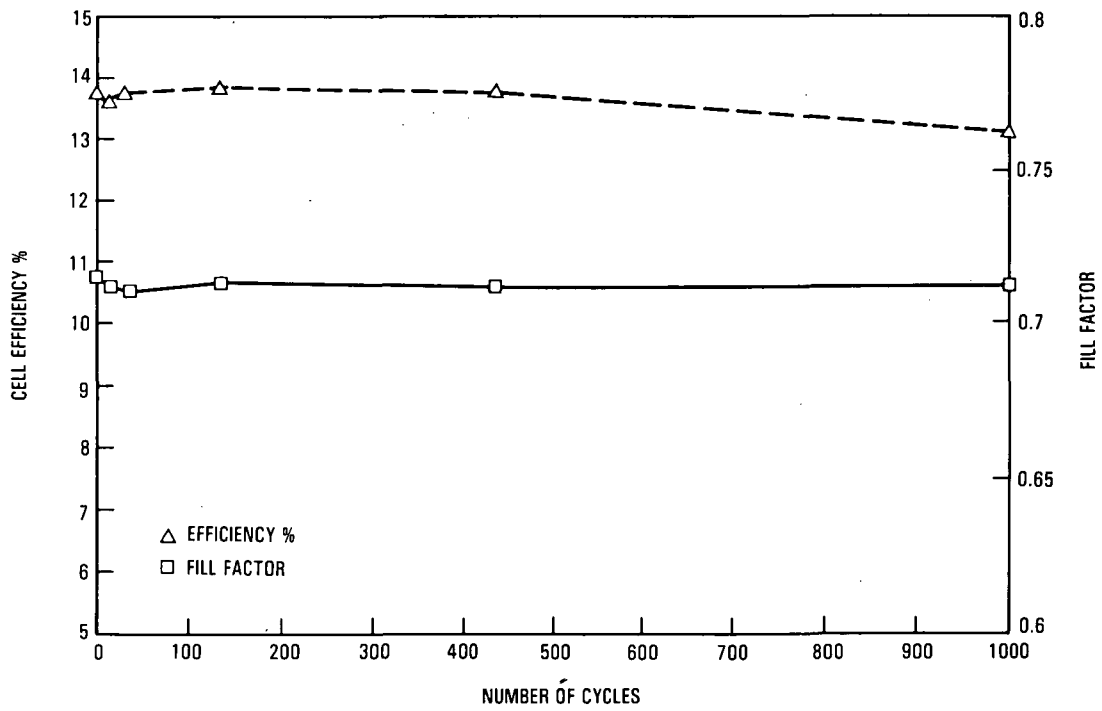


Figure 6-16. Temperature Cycling: Efficiency and Fill Factor Versus Number of Cycles, Cr/Pd/Ag

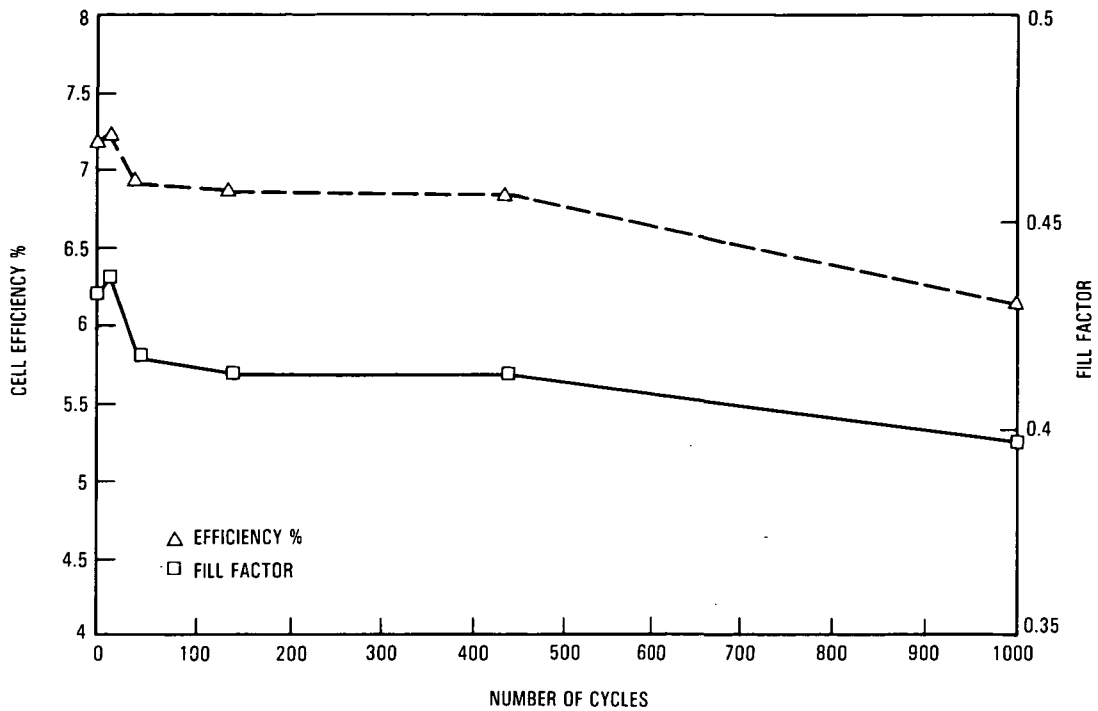


Figure 6-17. Temperature Cycling: Efficiency and Fill Factor Versus Number of Cycles, Thick Film Ag Paste

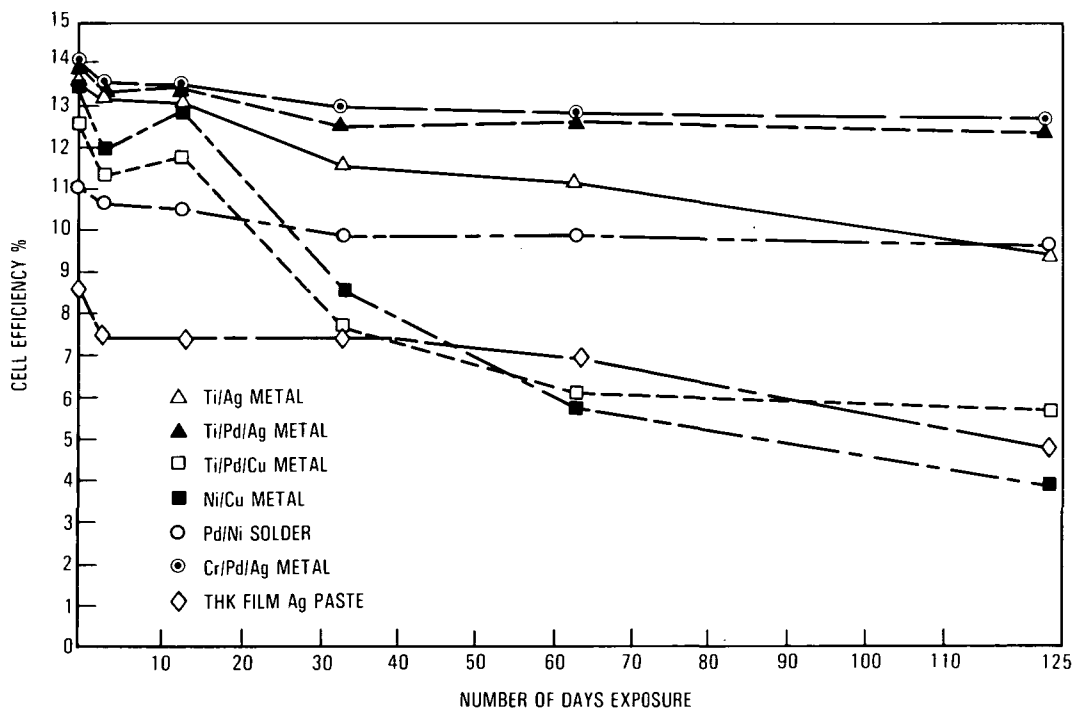


Figure 6-18. Humidity Tests: Efficiency Versus Number of Days Exposure For All Seven Metallization Systems

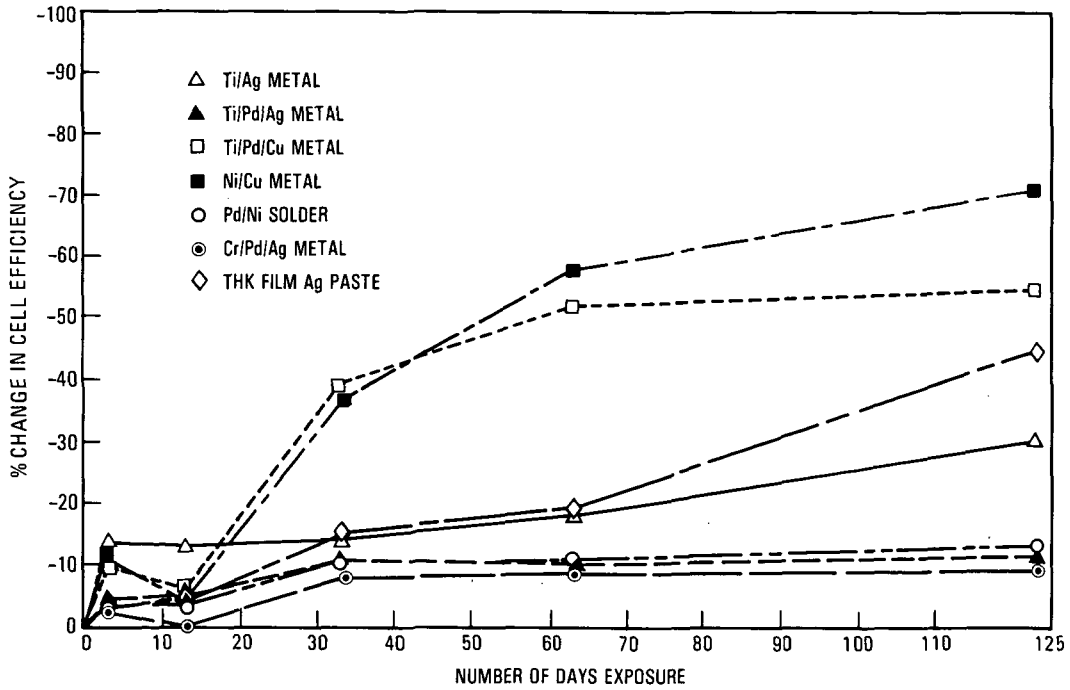


Figure 6-19. Humidity Tests: Percent Change in Efficiency Versus Number of Days Exposure For All Seven Metallization Systems

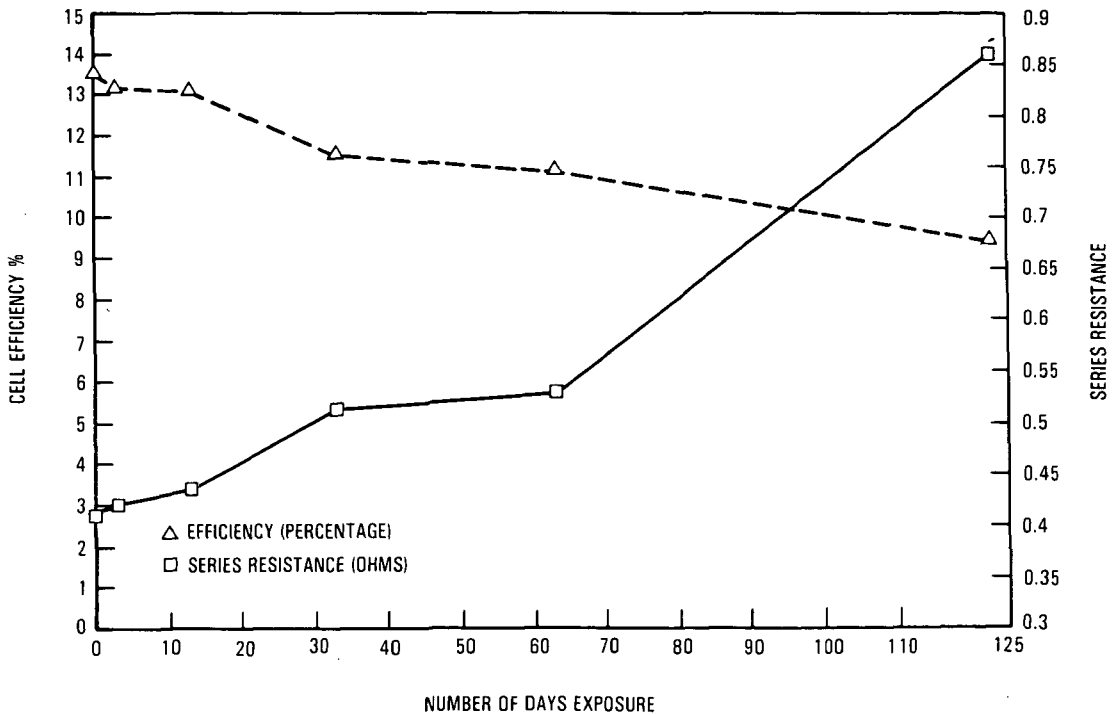


Figure 6-20. Humidity Tests: Efficiency and Series Resistance Versus Number of Days Exposure, Ti/Ag

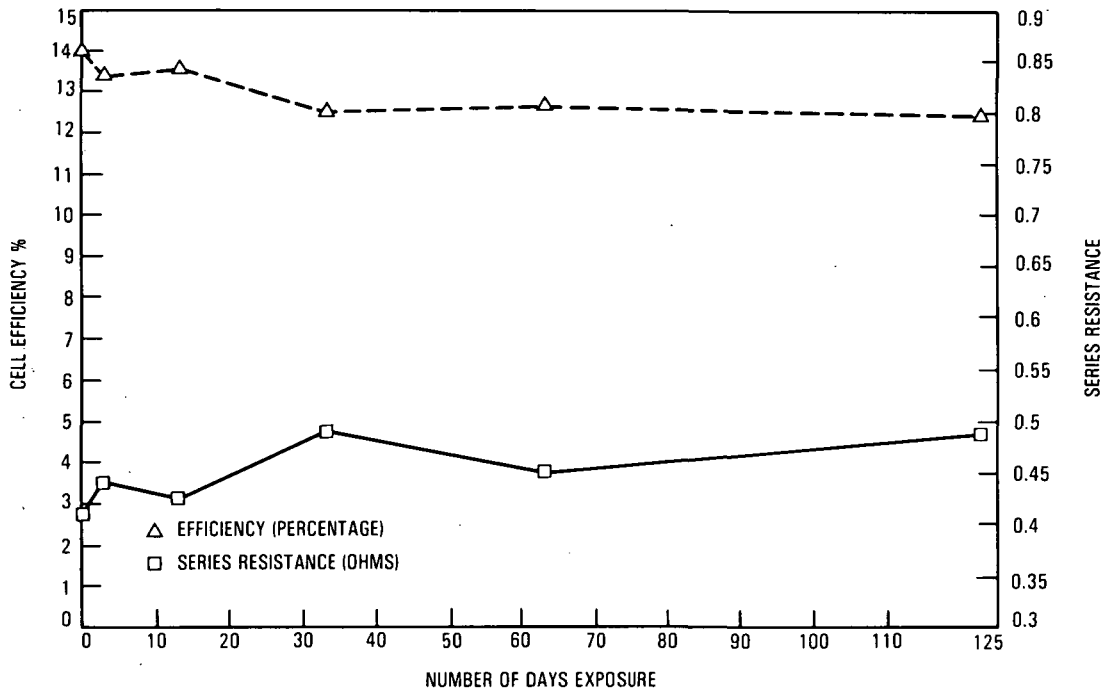


Figure 6-21. Humidity Tests: Efficiency and Series Resistance Versus Number of Days Exposure, Ti/Pd/Ag

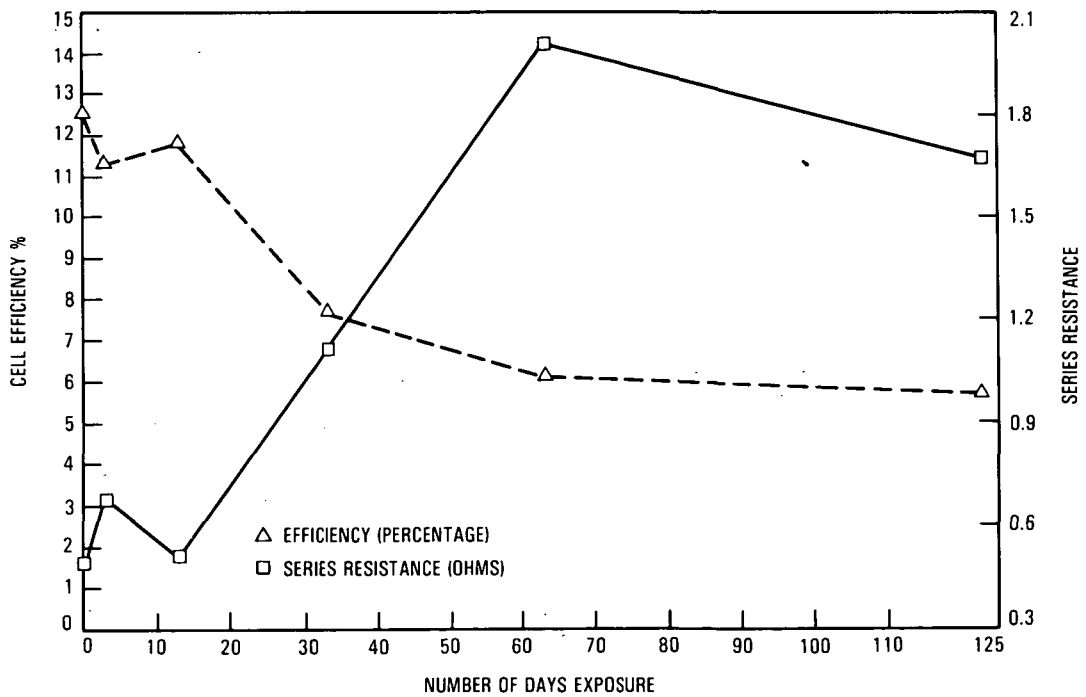


Figure 6-22. Humidity Tests: Efficiency and Series Resistance Versus Number of Days Exposure, Ti/Pd/Cu

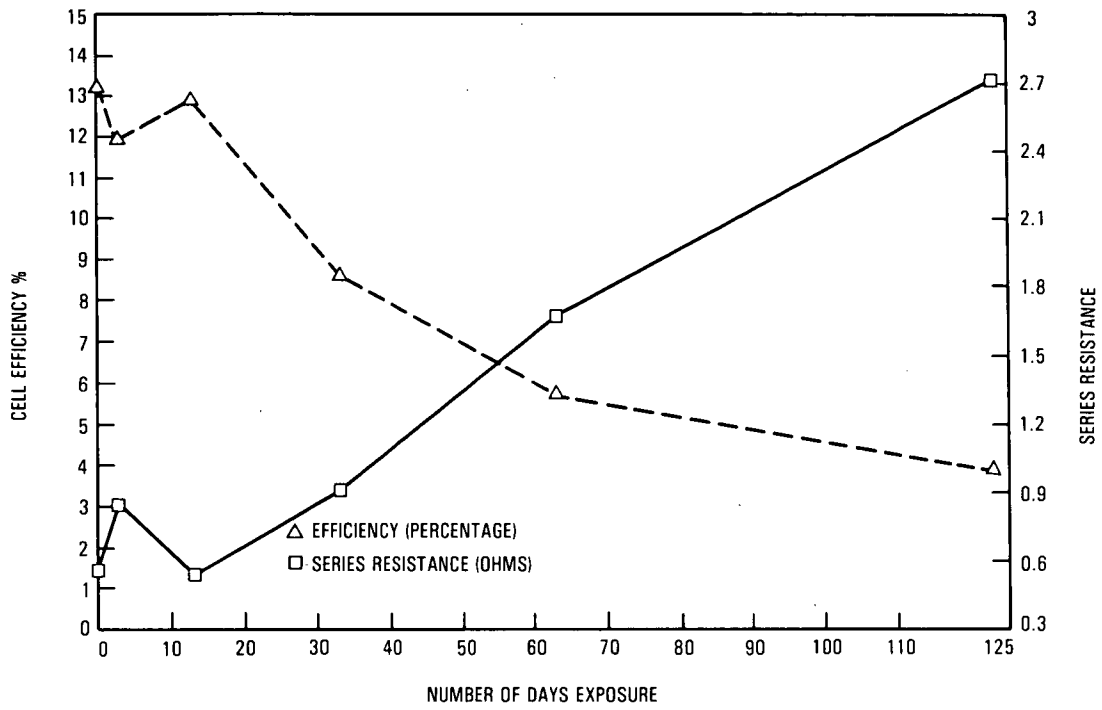


Figure 6-23. Humidity Tests: Efficiency and Series Resistance Versus Number of Days Exposure, Ni/Cu

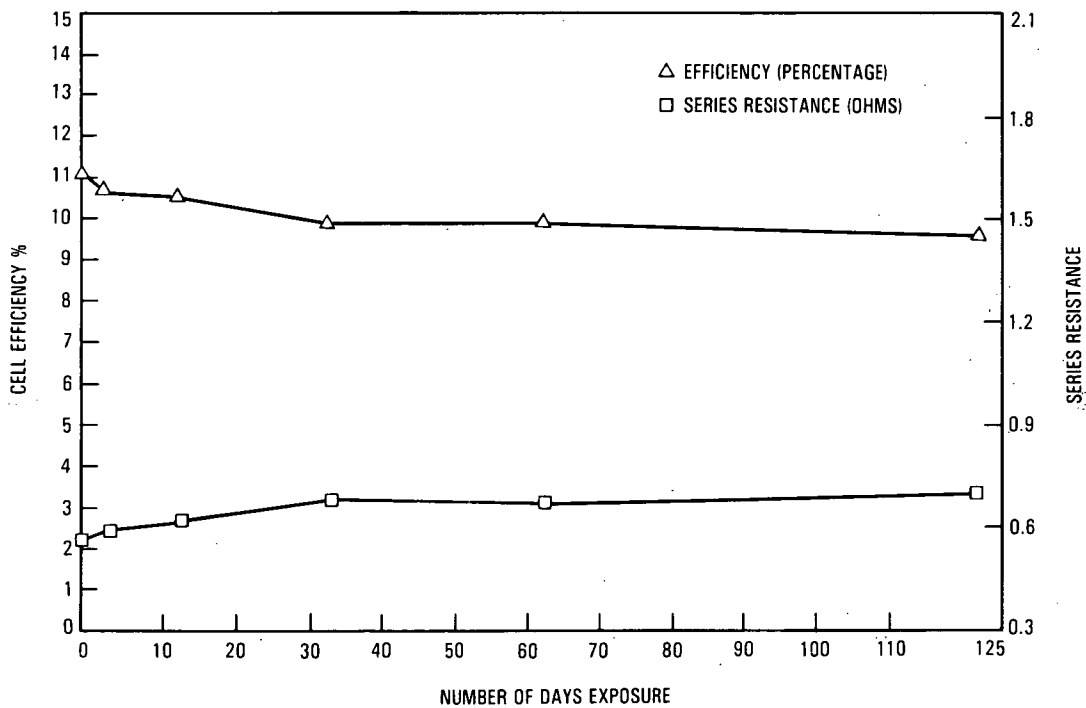


Figure 6-24. Humidity Tests: Efficiency and Series Resistance Versus Number of Days Exposure, Pd/Ni/Solder

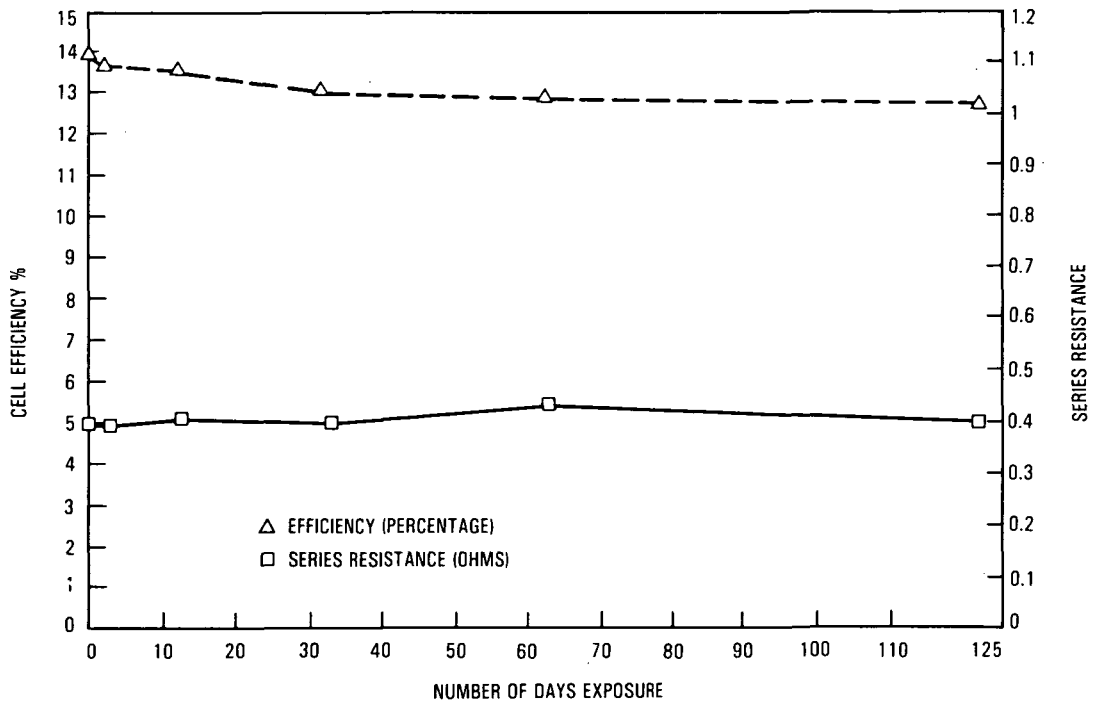


Figure 6-25. Humidity Tests: Efficiency and Series Resistance Versus Number of Days Exposure, Cr/Pd/Ag

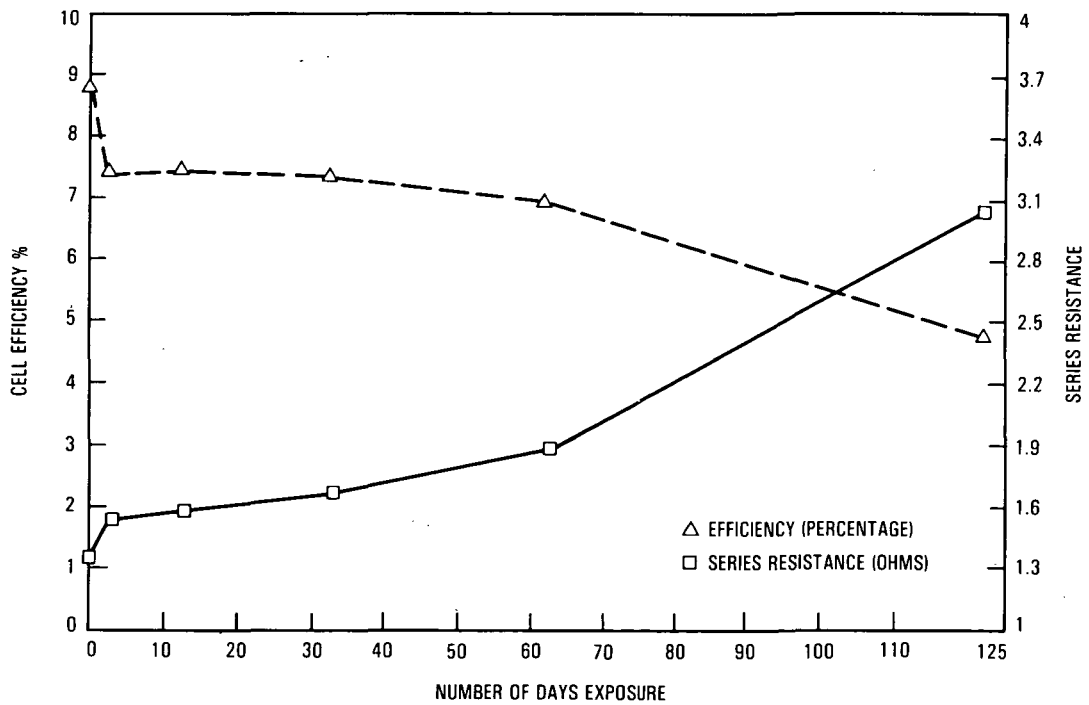


Figure 6-26. Humidity Tests: Efficiency and Series Resistance Versus Number of Days Exposure, Thick Film Ag Paste

B. SECONDARY ION MASS SPECTROMETRY EVALUATION

Three samples, one a control, one after 1000 temperature cycles, and one after 123 days humidity exposure, were taken from three metallization systems which were Ti/Ag, Ti/Pd/Ag, and Ti/Pd/Cu for a total of nine samples for oxygen content evaluation. The thinking was that if the moisture (water) from the humidity tests were absorbed into the metallization system, and if they reacted to form metal oxides, then an increase in oxygen content of the metallization system should be noted after exposure to humidity tests. A Secondary Ion Mass Spectrometer (SIMS) was used to determine oxygen content. The SIMS operates by boring small holes, 3 to 500 μm in diameter, down to a depth of 1 mil or less with a depth resolution of 100 to 200 \AA . The holes are bored by a beam of high-energy ions (5 to 20 keV) which erodes the material away, a small fraction of the eroded material being in the ionic form. The ionized material is then accelerated and passed through a mass spectrometer where it is analyzed for element identification and count.

Analysis of the SIMS depth profiles showed significant counts of H and O in the AR coatings on all three cell types, in all the environments, and in roughly the same concentrations. The H and O counts were assumed to be water. Similarly, no evidence of elevated oxygen concentration in the metallic layers were found after either temperature cycling or humidity exposures. The oxygen count was roughly the same for the control cells, the temperature-cycled cells, and the humidity-exposed cells. Figure 6-27 is a sample of the SIMS profile data that were generated.

The SIMS instrument cannot discern between bound oxygen (as in the case of metal oxides) or unbound oxygen (as in the case of trapped oxygen or oxygen agglomerates). It was surmised, however, that the unbound oxygen count in the metal layers were orders of magnitude larger and more variable than any bound oxygen, and swamped (or masked) any subtle changes in oxygen count due to metal oxide formation. It was concluded that the SIMS was not the proper instrument to determine metal oxide formation due to environmental exposures. No more measurements of the oxygen content of the metallization systems were pursued, because this type of effort was not a major thrust of the program.

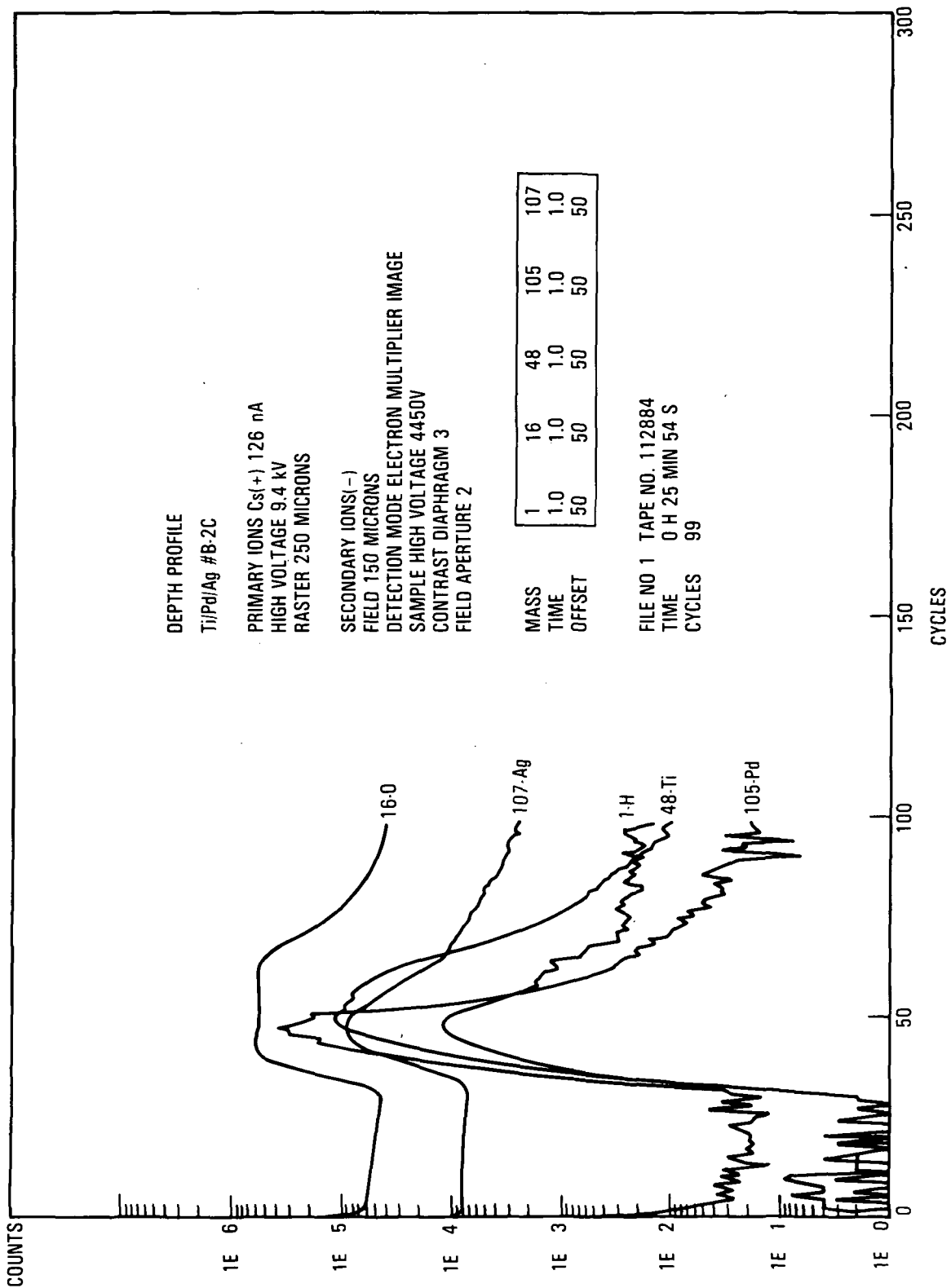


Figure 6-27. Sample of the SIMS Profile Data

C. I-V CURVES OF TEMPERATURE CYCLING AND HUMIDITY EXPOSURE TESTS

Tables 6-2 through 6-5 show the temperature cycling and humidity exposure test data that correspond to each of the three curves in each of the following figures. For example, the data in Table 6-2, under "A/Before Testing," correspond to Curve "A" in Figure 6-28; "B/After 440 Cycles," to Curve "B"; "C/After 1000 Cycles," to Curve "C."

Figures 6-28 through 6-31 show typical I-V curves of Ti/Pd/Ag and Ti/Pd/Cu metallization systems after subjection to temperature cycling tests and humidity exposure tests. As the I-V curves demonstrate, the Ti/Pd/Ag system held up well under the temperature cycling and humidity tests; the Ti/Pd/Cu did not perform well on either test.

Table 6-2. Data for I-V Curves of Temperature Cycling Test, Selected Sample, Ti/Pd/Cu

Ti/Pd/Cu Cell	Before Testing	After 440 Cycles	After 1000 Cycles
ID	B3-32	B3-32	B3-32
I_{sc}	127.9 mA	128.1 mA	123.4 mA
V_{oc}	585.0 mV	585.7 mV	587.0 mV
P_{mp}	46.6 mW	47.1 mW	36.5 mW
I_{mp}	110.8 mA	106.8 mA	94.0 mA
V_{mp}	420.4 mV	441.4 mV	389.0 mV
Efficiency	11.6%	11.8%	9.1%
Cell Area	4 sq cm	4 sq cm	4 sq cm
Fill Factor	0.622	0.627	0.504
R_s	0.551 ohms	0.469 ohms	1.318 ohms
R_{sh}	486.9 ohms	1315.5 ohms	315.3 ohms

I_{sc} = Short Circuit Current
 V_{oc} = Open Circuit Voltage
 P_{mp} = Maximum Power
 I_{mp} = Current at Maximum Power

V_{mp} = Voltage at Maximum Power
 R_s = Series Resistance
 R_{sh} = Shunt Resistance

Table 6-2 corresponds with Figure 6-28 on the following page.

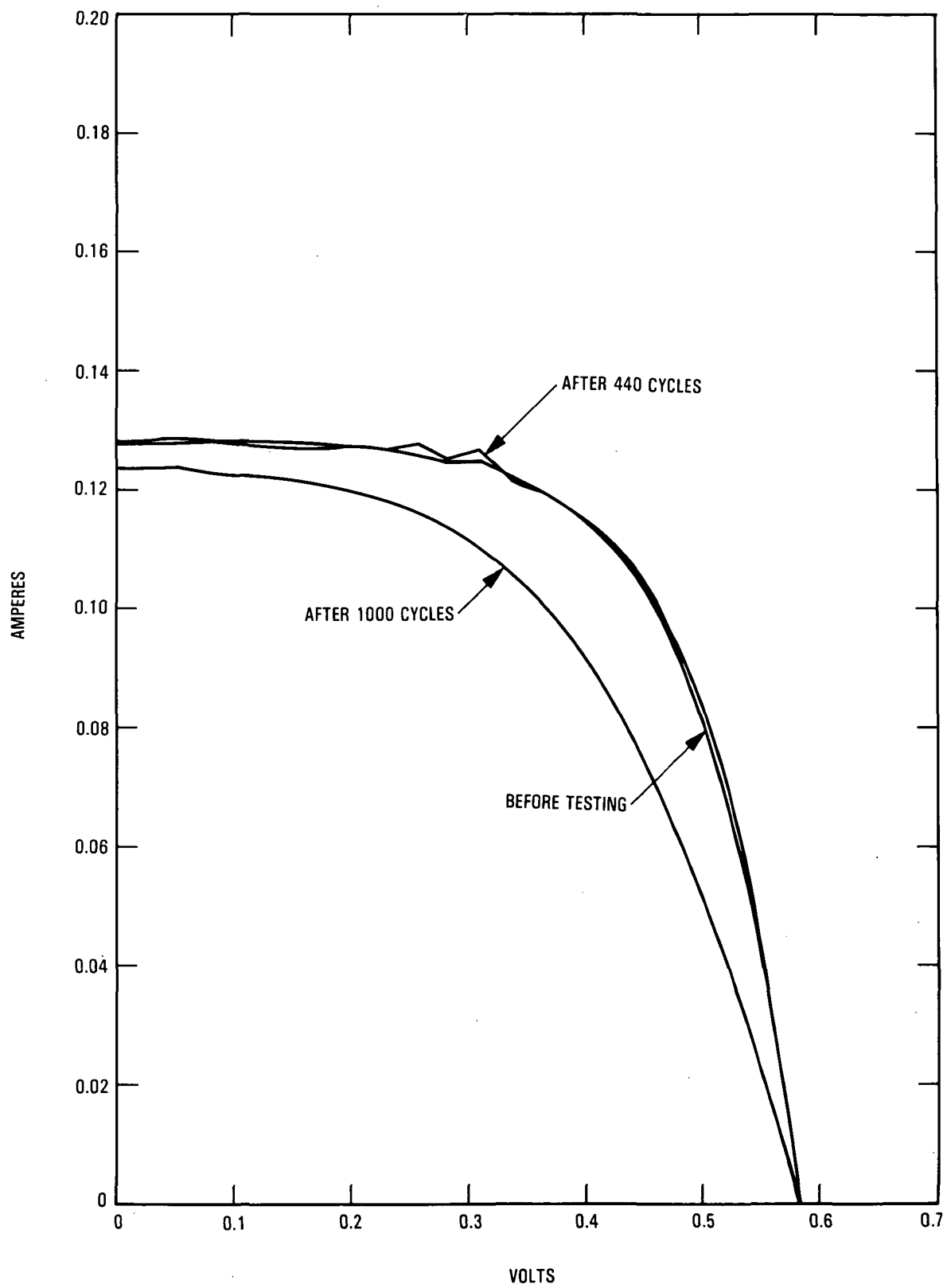


Figure 6-28. I-V Curves of Temperature Cycling Test, Selected Sample, Ti/Pd/Cu

Table 6-3. Data for I-V Curves of Temperature Cycling Test, Selected Sample, Ti/Pd/Ag

Ti/Pd/Ag Cell	Before Testing	After 440 Cycles	After 1000 Cycles
ID	B2-22	B2-22	B2-22
I_{sc}	130.2 mA	128.5 mA	124.8 mA
V_{oc}	593.8 mV	583.0 mV	587.0 mV
P_{mp}	56.8 mW	50.7 mW	50.0 mW
I_{mp}	118.3 mA	108.1 mA	105.5 mA
V_{mp}	480.0 mV	469.1 mV	473.6 mV
Efficiency	14.2%	12.7%	12.5%
Cell Area	4 sq cm	4 sq cm	4 sq cm
Fill Factor	0.734	0.677	0.682
R_s	0.413 ohms	0.422 ohms	0.416 ohms
R_{sh}	275.1 ohms	498.4 ohms	967.2 ohms

I_{sc} = Short Circuit Current
 V_{oc} = Open Circuit Voltage
 P_{mp} = Maximum Power
 I_{mp} = Current at Maximum Power

V_{mp} = Voltage at Maximum Power
 R_s = Series Resistance
 R_{sh} = Shunt Resistance

Table 6-3 corresponds with Figure 6-29 on the following page.

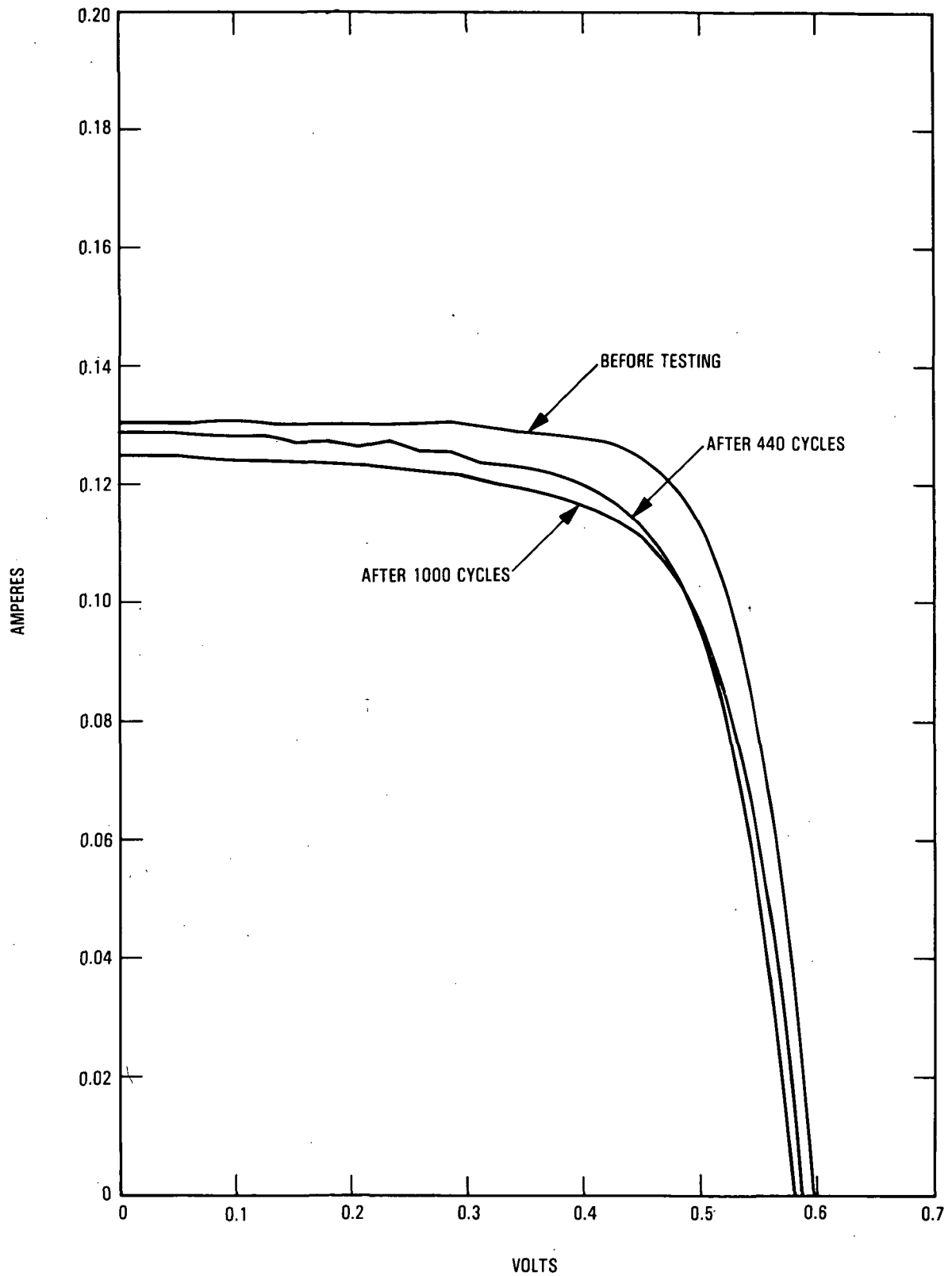


Figure 6-29. I-V Curves of Temperature Cycling Test, Selected Sample, Ti/Pd/Ag

Table 6-4. Data for I-V Curves of Humidity Exposure Test, Selected Sample, Ti/Pd/Cu

Ti/Pd/Cu Cell	Before Testing	After 13 Days	After 123 Days
ID	B3-21	B3-21	B3-21
I_{sc}	125.3 mA	123.5 mA	109.5 mA
V_{oc}	584.3 mV	577.4 mV	576.6 mV
P_{mp}	52.4 mW	48.9 mW	26.2 mW
I_{mp}	116.2 mA	110.5 mA	73.4 mA
V_{mp}	451.0 mV	442.7 mV	356.4 mV
Efficiency	13.1%	12.2%	6.5%
Cell Area	4 sq cm	4 sq cm	4 sq cm
Fill Factor	0.715	0.685	0.414
R_s	0.471 ohms	0.573 ohms	1.742 ohms
R_{sh}	229.0 ohms	183.4 ohms	20.3 ohms

I_{sc} = Short Circuit Current
 V_{oc} = Open Circuit Voltage
 P_{mp} = Maximum Power
 I_{mp} = Current at Maximum Power

V_{mp} = Voltage at Maximum Power
 R_s = Series Resistance
 R_{sh} = Shunt Resistance

Table 6-4 corresponds with Figure 6-30 on the following page.

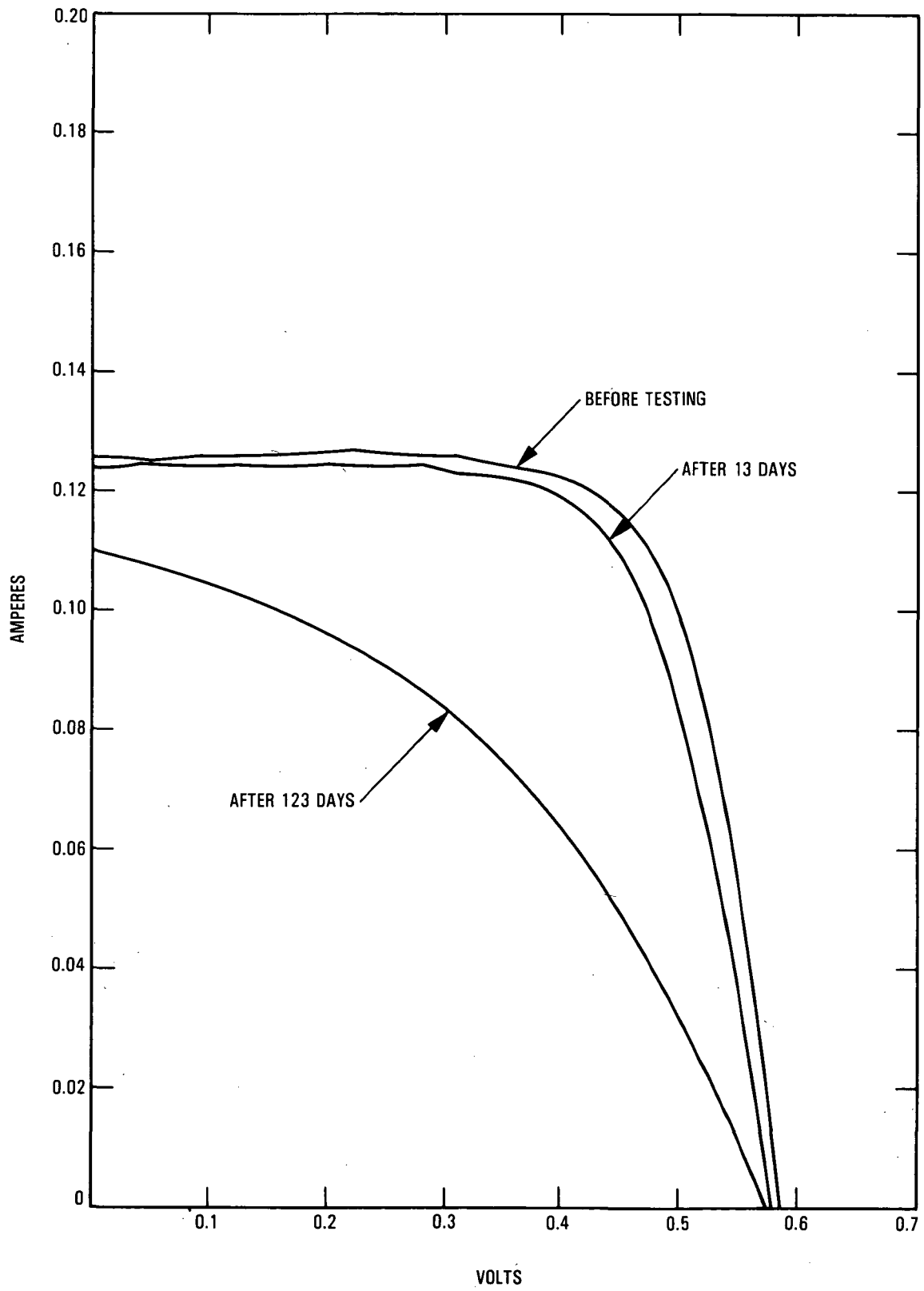


Figure 6-30. I-V Curves of Humidity Exposure Test, Selected Sample, Ti/Pd/Cu

Table 6-5. Data for I-V Curves of Humidity Exposure Test, Selected Sample, Ti/Pd/Ag

Ti/Pd/Ag Cell	Before Testing	After 13 Days	After 123 Days
ID	B2-5	B2-5	B2-5
I_{sc}	128.6 mA	126.0 mA	122.5 mA
V_{oc}	590.4 mV	565.6 mV	584.4 mV
P_{mp}	55.7 mW	51.8 mW	49.2 mW
I_{mp}	116.0 mA	110.3 mA	103.8 mA
V_{mp}	480.0 mV	469.7 mV	474.0 mV
Efficiency	13.9%	13.9%	12.3%
Cell Area	4 sq cm	4 sq cm	4 sq cm
Fill Factor	0.733	0.691	0.686
R_s	0.431 ohms	0.396 ohms	0.412 ohms
R_{sh}	202.5 ohms	106.9 ohms	242.5 ohms

I_{sc} = Short Circuit Current
 V_{oc} = Open Circuit Voltage
 P_{mp} = Maximum Power
 I_{mp} = Current at Maximum Power

V_{mp} = Voltage at Maximum Power
 R_s = Series Resistance
 R_{sh} = Shunt Resistance

Table 6-5 corresponds with Figure 6-31 on the following page.

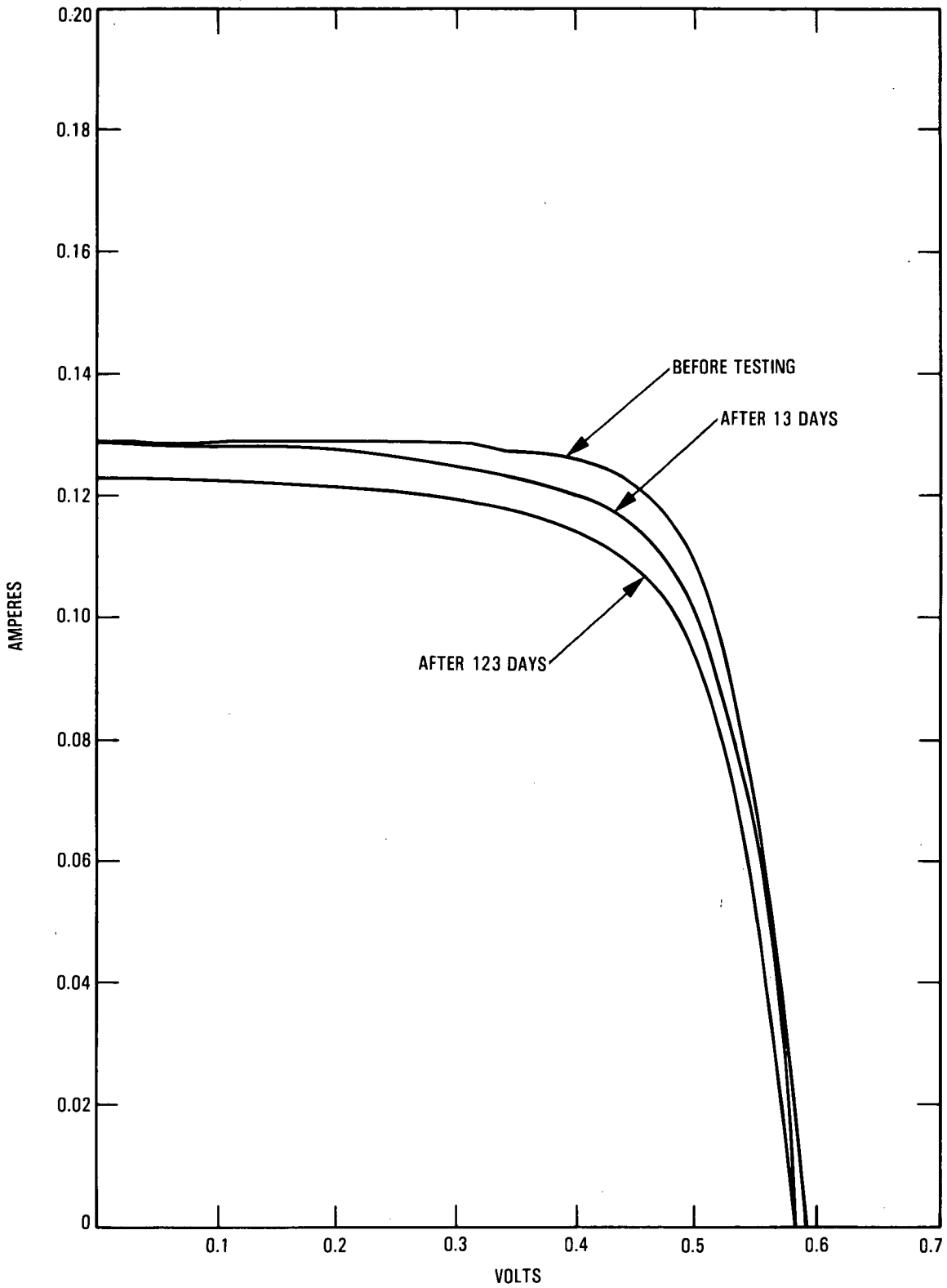


Figure 6-31. I-V Curves of Humidity Exposure Test, Selected Sample, Ti/Pd/Ag

SECTION VII

DISCUSSION OF RESULTS

A. OVERVIEW

There were no big surprises in the test results of the seven metallization systems after temperature cycling and humidity tests. A small surprise was that the Cr/Pd/Ag cell performed the best, i.e., showed the least degradation in cell efficiency after humidity tests, outperforming the highly touted Ti/Pd/Ag metallization system. The two systems, Cr/Pd/Ag and Ti/Pd/Ag, both performed considerably better than the other five systems. The Pd/Ni/Solder system performed respectably also. Not totally unexpected, the copper based systems performed the worst, in that they showed the most degradation in cell efficiency in both the temperature cycling and the humidity tests.

It should be pointed out that these test results do not necessarily rank metallization systems as to their ultimate use. Terrestrial cells are encapsulated and largely protected from the environment by an encapsulation system. There are studies in the FSA Project which investigated the environmental impact on encapsulated cells. The works of S. Shalaby (Reference 2) and J. Lathrop, et al. (Reference 3) address these areas. What this test program did was to present unencapsulated cell test data that show the relative vulnerabilities of different metallization systems to temperature cycling and humidity tests. The test program also isolated or separated unencapsulated cell data from encapsulated cell data, thereby enabling the researcher to identify specific variables which effect cell performance.

Regarding the poor performance of the copper based metal systems after humidity exposure, the question could be raised as to whether or not copper based metallization systems are suitable for terrestrial solar cells. The answer would be a qualified "yes." The test results suggest that copper based contact systems may need additional surface protection during shelf periods between cell completion and module fabrication. In large volume production, this shelf period could be several weeks or even months. A nickel or tin dip after copper plateup would suffice in giving surface protection to copper based systems.

B. TEMPERATURE CYCLING TESTS

On the temperature cycling tests, another one of the small, but pleasant, surprises was how reasonably well the temperature cycling tests matched with published data (References 3, 4, and 5). Six of the seven metallization systems showed a slight increase in cell efficiency, generally around 10 cycles, and then tapered off to a lower efficiency at the end

of 1,000 cycles. The Ti/Ag system showed the largest increase in efficiency (6.22%) and this occurred after 440 cycles. The one metallization system that showed no increase in cell efficiency, but a slow steady slight decline in efficiency at the end of 1,000 cycles, was Ti/Pd/Ag (3.69% decrease).

Firor and Hogan (Reference 6) show data on their thick film silver paste, solder dipped, that agree reasonably well with the Pd/Ni/Solder temperature cycling data of this program. Both curves of Reference 6 and this work show a slight increase in cell efficiency at 10 cycles followed by a slow decline in efficiency to a lower level than the starting efficiency after 30 cycles.

Discussions with space cell investigators indicate that they temperature cycle space modules for 20,000 cycles and more with little or no degradation in module efficiency. Because these space cells use Ti/Pd/Ag, a comparison with the Ti/Pd/Ag data might be made. The 3.69% decrease in cell efficiency of the Ti/Pd/Ag system in 1,000 cycles is statistically significant and seems to be at variance with space cell data which were reported verbally. The temperature excursions on space module testing can typically range from 100°C to -180°C for a delta T of 280°C. This compares with our 150°C to -65°C for a delta T of 215°C. There may be an alleviating effect on metallization stresses when cells are encapsulated.

A review of terrestrial module performance data (Reference 7) shows that terrestrial modules exhibit performance changes after temperature cycling. Twelve different mini-module types from different vendors were temperature cycled between 25 to 200 cycles at temperature ranges of +90°C to -40°C at 6 h/cycle. All of the mini-modules, after disallowing some mini-modules for obvious degradation reasons such as cracked cells, etc., still exhibited either a slight increase in power output (1 to 3%) or, in most cases, a slight decrease in power output (1 to 3%) after being subjected to 25 to 200 cycles (Reference 7 did not identify which mini-modules were subjected to the exact number of cycles). However, the mini-module data collectively showed similar behavior to the temperature cycling data of this test program, even though the temperature extremes and delta Ts were different, this program being the more severe with a delta T of 215°C versus their 130°C. A review of the temperature cycling curves in our tests show that within the first 200 cycles there is an overall slight decrease (1 to 3%) in cell efficiency with a slight increase occurring somewhere during the first 20 to 30 cycles, very much in agreement with the mini-module temperature cycling data (see Reference 7).

A review of the temperature cycling data in the Appendix shows that the V_{OC} remains (essentially) constant for all of the metallization systems during all of the 1,000 cycles. The significant changes occurred in the I_{SC} values and R_s (series resistance) values. This would infer that changes in the metallization system are occurring. Firor and Hogan (see Reference 4) indicate that the mechanical stress in metallization systems may be relieved by temperature excursions, some more than others. It is assumed that Firor

and Hogan meant mechanical stress at the metal-silicon interface. This seems to be the general assumption of most of the solar cell researchers and would explain the slight increases in cell efficiency after initial cycling tests. However, the steady fall-off in cell efficiency after continued temperature cycling may indicate a rebuilding of mechanical stress in the metal contact interfaces. Solar Cell Array Handbook (Reference 8) has a good section on fatigue of solar module components including cell interconnects, metal contacts, cell adhesion, etc.

J. Lathrop and others (see Reference 3) describe the results of their temperature cycling/temperature shock tests. Their bias-temperature data show remarkable similarity to the JPL temperature cycling data. Their bias temperature tests consisted of passing current through cells equal to approximately three times their use condition while subjecting the cells to temperatures at 75°, 135°C and 150°C. Their curves of solar cell power output versus exposure time showed a slight increase in power output initially (within the first 300 to 400 hours of testing), followed by a continuing decline in power output through 8000 hours of testing. This was true for three of their four metallization systems tested. Their Ti/Pd/Ag and a solder coated system both showed initial power output increase of 2 to 3% followed by a slight decrease of 2 to 3%, very similar in trend to the metallization systems in the temperature cycling tests of the JPL program. Lathrop and others (see Reference 3) also conducted temperature cycling/temperature shock tests. Their temperature extremes were the same as JPL's, from -65°C to +150°C. However, their cells were transferred (immediately) between two separate chambers each at one of the two temperature extremes, producing temperature failure modes, one involving lead-loss/cell fracture and the other mode involving gradual power loss. The JPL temperature cycling test, being much more gradual in reaching the temperature extremes (14 min ramp time between temperatures), also experienced several cell fractures during temperature cycling and exhibited overall decrease in power output after 1000 cycles.

C. DISCUSSION OF HUMIDITY TESTS

The results of the humidity tests were fairly predictable. As expected, because of the faster oxidation rate of copper, the copper based systems, Pd/Ni/Cu and Ni/Cu, performed the worst in that they exhibited the largest degradation in cell efficiencies of the seven metallization systems after 123 days of humidity exposure. All of the cells on all of the seven metallization systems showed evidence of blistering during humidity testing. Pictures of cells at 40x magnification after the total 123 days humidity exposure are shown herein. Bishop (Reference 9) presents a description of the mechanisms by which Ti/Ag contacts degrade. The model that he postulates to explain the degradation mechanism involves capillary condensation of water in the silver layer followed by electrochemical corrosion of the titanium. The reaction is assumed to be: $Ti + H_2O \longrightarrow TiO_2 + 2H_2$. It is believed by most researchers (including the author) that the tearing and blistering of the metal contacts is due to the release of hydrogen (or gaseous products) upon

oxidation of the metal under the metal surface. Bishop further develops the argument of oxidation under the metal surface by demonstrating that water can reach a silicon-silver interface through the silver under humidity conditions. After subjection to humidity conditions, water presence at the interface of silver coated silicon samples was determined by using internal reflection spectroscopy techniques involving reflection of infrared radiation through single crystal silicon. The presence of water was indicated at the interface by a decrease in transmission in the wave number region of 3400 cm^{-1} . The presence of water at the silicon-silver interface would provide the necessary catalyst for the degradation mechanism suggested by Bishop and others.

Becker and others (see Reference 10) looked at the silicon-titanium contact structure by the use of transmission electron microscopy techniques. They determined the presence of significant amounts of titanium hydride (TiH_2) at the contact interface and suggested the oxidation of the TiH_2 in the presence of water as a contributing factor in the formation of H_2 which leads to contact blisters and ultimate contact degradation. This is entirely plausible because many contact metals are normally sintered at 500 to 600°C in a forming gas of N_2/H_2 mixture. The Ti contacts used in this program were sintered in 100% N_2 and it is doubtful if any hydride was formed. Becker and others (see Reference 10) also indicated that the TiH_2 distribution in the Ti layers were highly uneven with some samples showing high TiH_2 concentrations while other samples showed little or no concentrations.

Becker and others (see Reference 10) indicated that they could not get a clear understanding of the oxygen behaviour of the Ti/Ag and Ti/Pd/Ag systems. This was due to the complex nature of oxide formations. Although the main thrust of this program was not to investigate degradation mechanisms, one of the interesting observations made was to determine the oxygen content of some of the metallization systems before and after environmental exposure. The thinking was that if the moisture (water) from the humidity tests was absorbed into the metallization system and reacted to form metal oxides, then an increase should be seen in oxygen content of the metallization system after exposure to humidity tests. A SIMS was used to determine oxygen content. The control sample, a 1000 temperature cycled sample, and a 123 day humidity exposed sample, were each tested for oxygen content from the Ti/Pd/Ag metallization system, the Ti/Ag system and the Pd/Ni/Cu metallization system (a total of nine samples tested). No significant differences could be found in oxygen content (count) in any of the samples. Because the SIMS cannot discern between bound oxygen (as in the case of metal oxides) and unbound oxygen (as in the case of trapped oxygen or oxygen agglomerates), it was surmised that the unbound oxygen count, being so much larger and variable, swamped (or masked) the subtle changes in oxygen count due to metal oxide formation. It was concluded that the SIMS was not the proper instrument to determine metal oxide formation in solar cells and that achieving a clear understanding about the oxygen behaviour of the metallization system was, indeed, as difficult a task as Becker (see Reference 10) alluded to. There were no further measurements of the oxygen content of the metallization systems, because this type of effort was not a major thrust of this program.

The summary remarks about this environmental test program are that: (1) it showed decided differences in the performances of different metallization systems after being subjected to environmental exposures; (2) these performance differences, however, did not rank the metallization system, as stated earlier, but did (and does) allow researchers to compare the relative sensitivities of different metallization systems to environmental exposures; (3) the test results showed remarkable agreement with other published results on environmental testing; and (4) the tabulated data in the Appendix should provide detailed information on cell performances after environmental exposures.

SECTION VIII

REFERENCES

1. Hoffman, A.R., Griffith, J.S., and Ross, R.G., "Qualification Testing of Flat-Plate Photovoltaic Modules," IEEE Transactions on Reliability, Vol. R-31, pp. 252-257, August 1982.
2. Shalaby, H., "The Degradation Mechanism of Ti-Pd-Ag Solar Cell Contacts by an Accelerated Electrochemical Testing Technique," Solar Cells, Vol. 11, pp. 189-193, 1984.
3. Lathrop, J.W., Hawkins, D.C., Prince, J.L., and Walker, H.A., "Accelerated Stress Testing of Terrestrial Solar Cells," IEEE Transactions on Reliability, Vol. R-31, pp. 258-265, August 1982.
4. Firor, K., and Hogan, S., "Environmental Testing of Single-Crystal Silicon Solar Cells with Screen-Printed Silver Contacts," IEEE Transactions on Reliability, Vol. R-31, pp. 271-275, August 1982.
5. Prince, J.L., Lathrop, J.L., and Whitter, G.W., "Contact Integrity Testing of Stress-Tested Silicon Terrestrial Solar Cells," Paper presented at 14th IEEE Photovoltaic Specialists Conference, San Diego, California, January 7-10, 1980. Conference Record (A81-27076 11-44), pp. 952-957, 1980.
6. Firor, K., and Hogan, B., "Effects of Processing Parameters on Thick Film Inks Used for Solar Cell Front Metallization," Solar Cells, Vol. 5, pp. 87-100, December 1981.
7. Maxwell, H.G., Grimmett, C.A., Repar, J., Frickland, P.O., and Amy, J.A. FSA Field Test Report 1980-1982, JPL Publication 83-29, Jet Propulsion Laboratory, Pasadena, California, April 15, 1983.
8. Rauschenbach, H.S., Solar Cell Array Design Handbook, Vols. 1 and 2, JPL Publication ST 43-38, Jet Propulsion Laboratory, Pasadena, California, October 1978.
9. Bishop, C.J., The Fundamental Mechanisms of Humidity Degradation in Silver Titanium Contacts, Paper presented at 8th IEEE Photovoltaic Specialists Conference, Seattle, Washington, August 4-6, 1970, pp. 51-61, AIAA 71A16061, August, 1970.
10. Becker, W.H., and Pollack, S.R., The Formation and Degradation of Ti-Ag and Ti-Pd-Ag Solar Cell Contacts, Paper presented at 8th IEEE Photovoltaic Specialists Conference, Seattle, Washington, August 4-6, 1970, pp. 40-50, AIAA 71A16060, August, 1970.

SECTION IX

SELECTED BIBLIOGRAPHY

- Aroian, L.A., Luft, W., and McCraven, C.C., "Temperature and Humidity Effects on Silicon Solar Cells," Paper presented at 7th Photovoltaic Specialists Conference, Pasadena, California, November 19-21, 1968. Conference Record (A69-35678 19-03), pp. 214-225, 1968.
- Berman, P., Mueller, R., and Solana, M., "Results of Accelerated Thermal Cycle Tests of Solar Cell Modules," Paper presented at 12th Photovoltaic Specialists Conference, Baton Rouge, Louisiana, November 15-18, 1976. Conference Record (A78-1090201-44), pp. 379-387, 1976.
- Boller, H.W., and Koch, J., "Accelerated Fatigue Tests of Solar Cell Interconnectors for Simulation of Thermal Cycles," Paper presented at 11th Photovoltaic Specialists Conference, Scottsdale, Arizona, May 6-8, 1975. Conference Record (A76-14727 04-44), pp. 153-161, 1975.
- Hoffman, A.R., and Ross, R.G., "Environmental Qualification Testing of Terrestrial Solar Cell Modules," Paper presented at 13th Photovoltaic Specialists Conference, Washington, D.C., June 5-8, 1978. Conference Record (A79-40881 17-44), pp. 835-842, 1978.
- Luft, W., "Silicon Solar Cells at Low Temperature," IEEE Transactions on Aerospace and Electronic Systems, Vol. AES-7, pp. 332-339, August, 1971.
- Luft, W., and Maiden, E., "Temperature Cycling Effects on Solar Panels," Paper presented at 4th Intersociety Energy Conversion Engineering Conference, Washington, D.C., September 22-26, 1969. Conference Record (A69-42236 23-03), pp. 582-589, September, 1969.
- Peterson, R.C., and Muled, A., "Silicon Solar Cells with Nickel/Solder Metallization," Proceedings of the Third International Photovoltaic Solar Energy Conference, Cannes, France, October 27-31, 1980. Conference Record (A82-24101 10-44), pp. 684-690, 1981.
- Smokler, M.I., and Runkle, L.O., "Experience in Design and Test of Terrestrial Solar-Cell Modules," Paper presented at AS/ISES 1982 Annual Meeting, Houston, Texas, June 1-5, 1982.

APPENDIX

Tables A-1 through A-14 present the JPL test data after temperature cycling and humidity exposure.

Table A-1. I-V Test Data After Temperature Cycling (Ti/Ag)^{a,b}

Cumulative No. of Temperature Cycles	Six Cells Total	I _{sc} (mA)	V _{oc} (mV)	P _{mp} (mW)	I _{mp} (mA)	V _{mp} (mV)	Eff (%)	Fill Factor (FF)	R _s (Series Resistance, ohms)	R _{sh} (Shunt Resistance, ohms)	% Change in Efficiency
0	Average	130.583	591.733	55.817	118.300	471.367	13.917	0.722	0.384	811.767	0
	Std. Dev.	1.579	2.736	2.938	3.092	14.240	0.734	0.031	0.034	964.789	
10	Average	130.117	591.083	55.583	118.683	468.217	13.900	0.722	0.409	650.333	-0.12
	Std. Dev.	1.945	2.486	2.874	4.345	10.761	0.737	0.028	0.028	676.285	
40	Average	130.233	591.950	55.550	118.417	469.050	13.900	0.720	0.405	339.583	-0.12
	Std. Dev.	2.641	2.689	3.678	6.472	10.742	0.916	0.034	0.036	93.119	
140	Average	130.800	591.950	55.300	119.150	463.450	13.833	0.713	0.436	362.950	-0.60
	Std. Dev.	2.574	2.545	4.145	5.633	14.305	1.031	0.040	0.068	349.047	
440	Average	130.400	589.200	55.183	120.117	463.100	14.783	0.718	0.466	236.567	+6.22
	Std. Dev.	1.457	2.265	2.628	4.544	13.444	2.019	0.030	0.125	62.189	
1000	Average	126.100	590.517	53.267	115.067	462.783	13.333	0.715	0.443	304.217	-4.20
	Std. Dev.	1.376	2.752	2.812	2.869	14.160	0.672	0.030	0.051	137.209	

^aTemperature excursions were:

From -65°C for approximately 6 min dwell at -65°C to +150°C for approximately 6 min dwell at +150°C, and approximately 14 min ramp time between temperatures. Total cycle time was approximately 40 min/cycle.

^bI-V test conditions were: AM1, 28°C

Table A-2. I-V Test Data After Temperature Cycling (Ti/Pd/Ag)^{a,b}

Cumulative No. of Temperature Cycles	Six Cells Total	I _{sc} (mA)	V _{oc} (mV)	P _{mp} (mW)	I _{mp} (mA)	V _{mp} (mV)	Eff (%)	Fill Factor (FF)	R _s (Series Resistance, ohms)	R _{sh} (Shunt Resistance, ohms)	% Change in Efficiency
0	Average	131.283	591.350	56.883	119.600	475.583	14.200	0.732	0.385	297.517	0
	Std. Dev.	1.158	1.590	1.191	0.913	10.640	0.289	0.020	0.022	80.181	
10	Average	130.233	590.750	56.033	119.517	487.717	14.017	0.727	0.406	380.867	-1.29
	Std. Dev.	1.064	2.376	1.872	1.943	45.621	0.460	0.024	0.026	188.084	
40	Average	130.340	590.540	56.580	119.400	473.940	14.080	0.735	0.414	380.280	-0.84
	Std. Dev.	1.650	3.433	1.418	2.772	0.952	0.397	0.009	0.039	319.765	
140	Average	131.160	590.500	55.920	119.600	467.300	14.000	0.721	0.402	204.720	-1.41
	Std. Dev.	1.375	3.199	2.871	3.566	11.720	0.713	0.032	0.024	60.521	
440	Average	130.650	588.325	56.750	120.075	472.625	13.850	0.739	0.459	477.175	-2.46
	Std. Dev.	0.743	2.124	0.634	1.291	0.414	0.166	0.006	0.158	307.766	
1000	Average	125.750	590.025	54.650	114.800	476.150	13.675	0.736	0.410	196.800	-3.70
	Std. Dev.	1.006	1.677	0.589	1.138	0.287	0.148	0.002	0.017	34.046	

^aTemperature excursions were: From -65°C for approximately 6 min dwell at -65°C to +150°C for approximately 6 min dwell at +150°C, and approximately 14 min ramp time between temperatures. Total cycle time was approximately 40 min/cycle.

^bIV test conditions were: AM1, 28°C

Table A-3. I-V Test Data After Temperature Cycling (Ti/Pd/Cu)^{a,b}

Cumulative No. of Temperature Cycles	Six Cells Total	I _{sc} (mA)	V _{oc} (mV)	P _{mp} (mW)	I _{mp} (mA)	V _{mp} (mV)	Eff (%)	Fill Factor (FF)	R _s (Series Resistance, ohms)	R _{sh} (Shunt Resistance, ohms)	% Change in Efficiency
0	Average	129.567	589.183	53.367	117.050	455.600	13.333	0.698	0.439	327.767	0
	Std. Dev.	1.314	2.929	3.252	3.538	20.079	0.832	0.035	0.058	134.246	
10	Average	130.017	589.767	53.683	115.833	463.000	13.417	0.699	0.451	426.333	+0.63
	Std. Dev.	1.038	1.685	2.992	3.645	13.599	0.727	0.033	0.035	201.607	
40	Average	130.350	588.800	50.267	116.100	432.567	12.583	0.654	0.653	342.917	-5.62
	Std. Dev.	1.393	2.049	2.945	4.050	14.047	0.736	0.042	0.143	137.856	
140	Average	130.733	590.267	53.700	116.000	462.550	13.417	0.695	0.442	342.250	+0.63
	Std. Dev.	1.064	1.730	3.049	3.968	13.536	0.767	0.034	0.039	107.660	
440	Average	129.917	586.000	52.700	114.067	461.767	13.167	0.692	0.454	510.950	-1.24
	Std. Dev.	1.218	2.879	2.987	3.885	13.483	0.736	0.036	0.057	380.920	
1000	Average	124.900	586.467	42.283	103.150	409.667	10.567	0.577	1.074	512.817	-20.74
	Std. Dev.	1.121	4.611	4.386	6.301	30.136	1.104	0.062	0.412	509.570	

^aTemperature excursions were:

From -65°C for approximately 6 min dwell at +150°C for approximately 6 min dwell at +150°C, and approximately 14 min ramp time between temperatures. Total cycle time was approximately 40 min/cycle.

^bIV test conditions were: AM1, 28°C

Table A-4. I-V Test Data After Temperature Cycling (Ni/Cu)^{a,b}

Cumulative No. of Temperature Cycles	Six Cells Total	I _{sc} (mA)	V _{oc} (mV)	P _{mp} (mW)	I _{mp} (mA)	V _{mp} (mV)	Eff (%)	Fill Factor (FF)	R _s (Series Resistance, ohms)	R _{sh} (Shunt Resistance, ohms)	% Change in Efficiency
0	Average	130.400	587.350	53.950	119.400	451.900	13.450	0.704	0.440	439.100	0
	Std. Dev.	0.400	0.950	0.550	1.100	0.400	0.150	0.006	0.036	42.000	
10	Average	130.800	588.700	55.000	116.450	472.200	13.750	0.714	0.453	207.250	+2.23
	Std. Dev.	0.400	0.900	0.300	0.550	0.200	0.050	0.004	0.002	60.550	
40	Average	131.200	588.600	53.000	118.750	446.650	13.250	0.686	0.572	200.500	-1.49
	Std. Dev.	0.200	1.600	0.600	1.350	0.050	0.150	0.007	0.023	23.500	
140	Average	131.350	587.700	52.400	117.800	445.000	13.100	0.678	0.575	278.400	-2.60
	Std. Dev.	0.450	1.700	1.000	2.000	0.600	0.200	0.012	0.029	87.400	
440	Average	130.400	587.750	51.950	116.900	444.550	12.950	0.678	0.591	228.750	-3.72
	Std. Dev.	0.300	0.250	2.650	1.100	26.750	0.650	0.036	0.135	37.350	
1000	Average	125.450	587.200	44.600	108.950	406.900	11.150	0.606	0.985	465.750	-17.10
	Std. Dev.	0.150	1.700	7.500	6.950	42.800	1.850	0.103	0.521	145.150	

^aTemperature excursions were:

From -65°C for approximately 6 min dwell at -65°C to +150°C for approximately 6 min dwell at +150°C, and approximately 14 min ramp time between temperatures. Total cycle time was approximately 40 min/cycle.

^bI-V test conditions were: AM1, 28°C

Table A-5. I-V Test Data After Temperature Cycling (Pd/Ni/Solder)^{a,b}

Cumulative No. of Temperature Cycles	Six Cells Total	I _{sc} (mA)	V _{oc} (mV)	P _{mp} (mW)	I _{mp} (mA)	V _{mp} (mV)	Eff (%)	Fill Factor (FF)	R _s (Series Resistance, ohms)	R _{sh} (Shunt Resistance, ohms)	% Change in Efficiency
0	Average	123.150	578.000	42.867	104.667	409.300	10.717	0.602	0.581	1227.183	0
	Std. Dev.	0.930	6.372	2.698	4.754	13.717	0.664	0.035	0.036	1117.428	
10	Average	125.350	581.617	43.350	106.750	406.183	10.867	0.594	0.583	425.350	+1.40
	Std. Dev.	0.714	4.817	2.345	3.972	12.946	0.579	0.032	0.043	105.834	
40	Average	125.800	580.933	43.000	106.683	402.867	10.750	0.589	0.601	567.283	+0.30
	Std. Dev.	1.667	4.018	2.179	2.827	13.890	0.538	0.034	0.058	279.860	
140	Average	126.400	580.833	40.733	104.650	387.033	10.183	0.554	0.769	389.100	-4.98
	Std. Dev.	1.271	5.078	6.308	6.612	40.127	1.591	0.084	0.426	257.060	
440	Average	125.500	578.283	41.817	104.417	400.267	10.500	0.576	0.595	573.117	-2.02
	Std. Dev.	1.153	5.936	3.155	5.005	14.451	0.688	0.040	0.056	519.443	
1000	Average	121.483	577.383	39.867	99.683	399.650	9.967	0.568	0.616	2862.317	-7.00
	Std. Dev.	0.869	3.544	2.535	4.090	13.233	0.621	0.036	0.053	5577.968	

^a Temperature excursions were:
 From -65°C for approximately 6 min dwell at +150°C for approximately 6 min dwell at +150°C, and approximately 14 min ramp time between temperatures. Total cycle time was approximately 40 min/cycle.
^b I-V test conditions were: AM1, 28°C

Table A-6. I-V Test Data After Temperature Cycling (Thick Film Ag Paste)^{a,b}

Cumulative No. of Temperature Cycles	Six Cells Total	I _{sc} (mA)	V _{oc} (mV)	P _{mp} (mW)	I _{mp} (mA)	V _{mp} (mV)	Eff (%)	Fill Factor (FF)	R _s (Series Resistance, ohms)	R _{sh} (Shunt Resistance, ohms)	% Change in Efficiency
0	Average	114.167	578.617	28.600	77.917	363.050	7.167	0.432	1.316	23.067	0
	Std. Dev.	4.140	2.669	6.562	7.628	53.263	1.630	0.092	0.554	9.740	
10	Average	114.380	578.400	28.820	78.920	364.000	7.240	0.436	1.295	24.220	+1.02
	Std. Dev.	6.823	4.370	5.688	8.688	47.754	1.424	0.081	0.469	9.808	
40	Average	114.600	577.560	27.720	79.060	348.500	6.900	0.417	1.444	22.040	-3.72
	Std. Dev.	5.912	2.525	6.490	10.955	50.830	1.616	0.087	0.505	9.156	
140	Average	114.120	578.440	27.440	77.360	352.020	6.860	0.413	1.499	20.680	-4.28
	Std. Dev.	8.284	1.679	6.829	10.914	52.599	1.707	0.087	0.508	7.791	
440	Average	113.620	579.620	27.380	77.340	351.660	6.840	0.413	1.514	21.360	-4.56
	Std. Dev.	9.073	1.975	6.822	13.377	46.263	1.693	0.087	0.502	9.095	
1000	Average	107.160	578.100	24.620	72.220	339.260	6.140	0.397	1.929	18.560	-14.33
	Std. Dev.	7.927	2.923	5.058	7.874	41.304	1.245	0.071	0.655	3.237	

^aTemperature excursions were:
From -65°C for approximately 6 min dwell at -65°C to +150°C for approximately 6 min dwell at +150°C, and approximately 14 min ramp time between temperatures. Total cycle time was approximately 40 min/cycle.

^bIV test conditions were: AM1, 28°C

Table A-7. I-V Test Data After Temperature Cycling (Cr/Pd/Ag)^{a, b}

Cumulative No. of Temperature Cycles	Six Cells Total	I _{sc} (mA)	V _{oc} (mV)	P _{mp} (mW)	I _{mp} (mA)	V _{mp} (mV)	Eff (%)	Fill Factor (FF)	R _s (Series Resistance, ohms)	R _{sh} (Shunt Resistance, ohms)	% Change in Efficiency
0	Average	130.833	588.400	55.083	117.083	470.183	13.767	0.715	0.418	283.267	0
	Std. Dev.	1.216	3.426	2.540	2.839	13.907	0.605	0.027	0.032	98.764	
10	Average	129.983	586.683	54.317	117.083	463.600	13.583	0.712	0.432	374.417	-1.33
	Std. Dev.	2.193	4.160	2.796	3.149	13.560	0.722	0.029	0.035	371.628	
40	Average	131.700	588.467	54.933	119.250	460.717	13.750	0.709	0.421	923.300	-0.123
	Std. Dev.	1.547	3.723	2.749	3.495	13.915	0.665	0.031	0.034	1202.774	
140	Average	132.000	588.217	55.367	119.383	463.617	13.833	0.713	0.414	238.217	+0.48
	Std. Dev.	1.179	3.392	2.769	2.807	13.455	0.692	0.030	0.018	100.856	
440	Average	131.350	587.433	54.917	118.533	463.050	13.733	0.711	0.418	348.217	-0.25
	Std. Dev.	1.355	3.065	2.687	2.857	13.379	0.680	0.029	0.035	170.960	
1000	Average	125.833	585.683	52.533	114.617	458.250	13.133	0.712	0.427	278.417	-4.6
	Std. Dev.	1.217	3.124	2.502	4.125	12.854	0.639	0.029	0.037	59.742	

^aTemperature excursions were:
From -65°C for approximately 6 min dwell at -65°C to +150°C for approximately 6 min dwell at +150°C, and approximately 14 min ramp time between temperatures. Total cycle time was approximately 40 min/cycle.

^bIV test conditions were: AM1, 28°C

Table A-8. I-V Test Data After Humidity Tests (Ti/Ag) a,b

Cumulative No. of Days Exposure to Humidity	Six Cells Total	I _{sc} (mA)	V _{oc} (mV)	P _{mp} (mW)	I _{mp} (mA)	V _{mp} (mV)	Eff (%)	Fill Factor (FF)	R _s (Series Resistance, ohms)	R _{sh} (Shunt Resistance, ohms)	% Change in Cell Efficiency
0	Average	130.994	588.133	54.067	115.733	467.222	13.522	0.701	0.414	1080.344	0
	Std. Dev.	1.972	4.866	2.997	5.198	14.418	0.744	0.034	0.038	2500.552	
3	Average	129.922	585.167	52.633	113.711	462.778	13.144	0.692	0.422	240.011	-2.80
	Std. Dev.	1.496	3.138	2.685	4.001	13.126	0.675	0.030	0.029	88.434	
13	Average	130.078	585.578	52.300	111.244	469.933	13.056	0.686	0.436	269.211	-3.45
	Std. Dev.	2.254	3.456	3.201	6.403	1.856	0.818	0.032	0.031	155.320	
33	Average	123.811	581.333	46.011	103.822	442.678	11.522	0.638	0.514	282.244	-14.79
	Std. Dev.	2.595	4.273	3.837	6.898	9.878	0.959	0.045	0.058	270.799	
63	Average	123.033	581.989	44.511	101.322	438.833	11.133	0.621	0.529	387.622	-17.67
	Std. Dev.	3.358	3.401	4.427	8.325	12.361	1.115	0.053	0.062	316.881	
123	Average	120.689	582.567	37.789	91.233	411.367	9.444	0.535	0.861	530.844	-30.16
	Std. Dev.	3.771	2.963	6.415	7.920	35.806	1.604	0.076	0.375	822.928	

^a Humidity conditions were: 60°C at 100% saturation for first 13 days and 70°C at 98% Relative Humidity for 14 through 123 days. The reason for the variance in test conditions was because the cell specimens were tested piggyback with other specimens on other programs which had priority on the test conditions.

^b IV test conditions were: AML, 28°C

Table A-9. I-V Test Data After Humidity Tests (Ti/Pi/Ag) ^{a,b}

Cumulative No. of Days Exposure to Humidity	Six Cells Total	I _{sc} (mA)	V _{oc} (mV)	P _{mp} (mW)	I _{mp} (mA)	V _{mp} (mV)	Eff (%)	Fill Factor (FF)	R _s (Series Resistance, ohms)	R _{sh} (Shunt Resistance, ohms)	% Change in Cell Efficiency
0	Average	130.267	590.556	55.988	118.933	470.811	14.000	0.727	0.411	257.356	0
	Std. Dev.	1.194	2.276	1.109	3.029	12.911	0.279	0.014	0.020	71.486	
3	Average	128.344	586.856	53.456	116.167	460.422	13.367	0.709	0.441	364.556	-4.52
	Std. Dev.	1.480	2.726	2.162	4.411	13.083	0.540	0.023	0.039	187.134	
13	Average	129.289	587.389	54.178	115.344	468.244	13.544	0.712	0.425	600.244	-3.26
	Std. Dev.	1.440	1.849	2.171	4.588	8.029	0.534	0.024	0.032	835.344	
33	Average	123.267	583.644	49.922	110.011	454.156	12.478	0.694	0.490	327.156	-10.87
	Std. Dev.	1.551	1.864	2.075	3.527	16.662	0.533	0.035	0.107	206.946	
63	Average	123.278	584.056	50.400	109.033	462.367	12.600	0.700	0.450	1444.756	-10.00
	Std. Dev.	1.319	1.424	2.376	4.341	13.264	0.600	0.035	0.053	3016.517	
123	Average	122.900	583.489	49.567	108.967	454.422	12.411	0.691	0.487	288.487	-11.35
	Std. Dev.	0.814	1.458	4.094	4.571	25.574	1.018	0.055	0.144	101.762	

^a Humidity conditions were:

60°C at 100% saturation for first 13 days and 70°C at 98% Relative Humidity for 14 through 123 days. The reason for the variance in test conditions was because the cell specimens were tested piggyback with other specimens on other programs which had priority on the test conditions.

^b I-V test conditions were: AM1, 28°C

Table A-10. I-V Test Data After Humidity Tests (Ti/Pd/Cu)^{a,b}

Cumulative No. of Days Exposure to Humidity	Six Cells Total	I _{sc} (mA)	V _{oc} (mV)	P _{mp} (mW)	I _{mp} (mA)	V _{mp} (mV)	Eff (%)	Fill Factor (FF)	R _s (Series Resistance, ohms)	R _{sh} (Shunt Resistance, ohms)	% Change in Cell Efficiency
0	Average	128.689	584.256	50.222	111.044	449.011	12.533	0.665	0.486	848.111	0
	Std. Dev.	2.966	6.698	7.993	11.038	35.945	2.004	0.096	0.130	1384.937	
3	Average	125.667	581.178	45.211	105.000	427.067	11.300	0.617	0.688	274.889	-9.83
	Std. Dev.	3.132	5.952	8.063	10.755	42.907	2.005	0.105	0.288	180.793	
13	Average	126.744	580.878	47.156	105.389	444.289	11.789	0.638	0.514	284.000	-5.94
	Std. Dev.	2.683	5.649	7.751	11.240	35.138	1.923	0.096	0.074	162.539	
33	Average	112.789	573.222	30.578	80.611	373.244	7.633	0.463	1.117	99.867	-39.10
	Std. Dev.	17.072	12.066	9.348	18.298	43.550	2.337	0.093	0.575	119.413	
63	Average	101.628	568.671	24.371	69.957	339.214	6.086	0.408	2.004	31.986	-51.44
	Std. Dev.	22.140	16.167	8.560	19.057	33.782	2.115	0.064	0.817	19.586	
123	Average	97.633	566.200	22.833	63.689	350.578	5.711	0.402	1.672	21.533	-54.43
	Std. Dev.	19.186	18.514	7.248	14.900	38.628	1.806	0.056	0.734	8.632	

^aHumidity conditions were:

60°C at 100% saturation for first 13 days and 70°C at 98% Relative Humidity for 14 through 123 days. The reason for the variance in test conditions was because the cell specimens were tested piggyback with other specimens on other programs which had priority on test conditions.

^bI-V test conditions were: AM1, 28°C.

Table A-11. I-V Test Data After Humidity Tests (Ni/Cu)^{a,b}

Cumulative No. of Days Exposure to Humidity	Six Cells Total	I _{sc} (mA)	V _{oc} (mV)	P _{mp} (mW)	I _{mp} (mA)	V _{mp} (mV)	E _{ff} (%)	Fill Factor (FF)	R _s (Series Resistance, ohms)	R _{sh} (Shunt Resistance, ohms)	% Change in Cell Efficiency
0	Average	131.467	591.700	53.667	118.900	451.533	13.400	0.689	0.559	146.900	0
	Std. Dev.	0.694	0.942	2.034	4.182	1.228	0.608	0.022	0.093	29.087	
3	Average	129.367	588.600	47.667	114.200	417.433	11.900	0.625	0.858	424.100	-11.19
	Std. Dev.	0.368	1.478	0.759	1.705	0.450	0.216	0.007	0.038	275.770	
13	Average	128.900	586.800	51.533	115.967	444.267	12.900	0.680	0.541	272.200	-3.73
	Std. Dev.	1.846	2.412	1.506	3.205	0.873	0.374	0.014	0.053	88.583	
33	Average	112.100	580.400	34.167	82.533	412.933	8.567	0.520	0.909	91.633	-36.07
	Std. Dev.	14.799	5.102	6.925	15.907	4.712	1.763	0.039	0.089	84.532	
63	Average	92.067	576.733	22.700	59.767	378.800	5.700	0.425	1.666	22.933	-57.46
	Std. Dev.	21.532	6.246	5.838	14.699	4.287	1.470	0.019	0.293	5.074	
123	Average	73.667	567.433	15.500	47.300	330.667	3.867	0.374	2.718	20.100	-71.14
	Std. Dev.	17.020	5.961	3.253	10.881	32.291	0.801	0.034	0.733	6.505	

^aHumidity conditions were: 60°C at 100% saturation for first 13 days and 70°C at 98% Relative Humidity for 14 through 123 days. The reason for the variance in test conditions was because the cell specimens were tested piggyback with other specimens on other programs which had priority on test conditions.

^bIV test conditions were: AM1, 28°C

Table A-12. I-V Test Data After Humidity Tests (Pd/Ni/Solder) ^{a,b}

Cumulative No. of Days Exposure to Humidity	Six Cells Total	I _{sc} (mA)	V _{oc} (mV)	P _{mp} (mW)	I _{mp} (mA)	V _{mp} (mV)	Eff (%)	Fill Factor (FF)	R _s (Series Resistance, ohms)	R _{sh} (Shunt Resistance, ohms)	% Change in Cell Efficiency
0	Average	124.133	577.889	44.233	107.778	410.267	11.056	0.616	0.569	660.778	0
	Std. Dev.	0.738	2.396	2.150	2.659	13.783	0.529	0.032	0.058	794.566	
3	Average	123.078	575.289	42.489	105.456	403.056	10.633	0.600	0.597	2050.033	-3.83
	Std. Dev.	1.863	2.688	2.640	5.449	13.504	0.673	0.034	0.052	4687.784	
13	Average	120.967	575.489	41.233	101.833	404.167	10.500	0.590	0.625	466.400	-5.03
	Std. Dev.	4.591	3.652	4.387	8.933	13.885	0.720	0.047	0.096	514.583	
33	Average	116.756	577.233	38.733	96.922	399.144	9.878	0.576	0.684	790.322	-10.65
	Std. Dev.	4.379	7.534	4.206	8.238	18.658	0.725	0.050	0.136	1065.202	
63	Average	116.565	574.800	38.844	96.689	401.644	9.900	0.579	0.672	421.067	-10.46
	Std. Dev.	4.461	3.026	3.995	8.658	13.859	0.618	0.045	0.090	226.738	
123	Average	112.156	571.889	36.444	92.200	395.044	9.622	0.567	0.704	429.900	-12.97
	Std. Dev.	10.148	3.072	5.127	12.278	10.931	0.611	0.047	0.125	505.046	

^a Humidity conditions were: 60°C at 100% saturation for first 13 days and 70°C at 98% Relative Humidity for 14 through 123 days. The reason for the variance in test conditions was because the cell specimens were tested piggyback with other specimens on other programs which had priority on the test conditions.

^b IV test conditions were: AM1, 28°C

Table A-13. I-V Test Data After Humidity Tests (Cr/Pd/Ag)^{a,b}

Cumulative No. of Days Exposure to Humidity	Six Cells Total	I _{sc} (mA)	V _{oc} (mV)	P _{mp} (mW)	I _{mp} (mA)	V _{mp} (mV)	Eff (%)	Fill Factor (FF)	R _s (Series Resistance, ohms)	R _{sh} (Shunt Resistance, ohms)	% Change in Cell Efficiency
0	Average	130.389	590.600	56.267	118.000	476.900	14.056	0.730	0.399	10903.889	0
	Std. Dev.	2.574	2.780	1.652	2.329	9.075	0.430	0.020	0.030	29778.329	
3	Average	128.578	586.656	54.311	115.789	469.100	13.589	0.720	0.395	1384.389	-3.32
	Std. Dev.	3.766	2.980	2.644	5.090	8.466	0.666	0.020	0.021	1584.351	
13	Average	128.667	586.667	54.056	115.389	468.422	13.511	0.715	0.409	447.067	-3.88
	Std. Dev.	3.633	2.586	2.371	4.741	8.323	0.612	0.018	0.019	490.354	
33	Average	123.322	583.811	51.800	109.722	472.11	12.956	0.719	0.398	385.411	-7.83
	Std. Dev.	3.440	2.070	2.291	4.616	8.279	0.574	0.017	0.022	304.854	
63	Average	123.422	584.444	51.400	110.456	465.811	12.856	0.712	0.433	3630.944	-8.54
	Std. Dev.	3.283	1.640	2.335	4.509	17.579	0.583	0.026	0.104	9352.993	
123	Average	121.700	582.378	50.922	108.522	469.122	12.744	0.718	0.404	753.889	-9.33
	Std. Dev.	2.816	1.721	1.997	3.279	11.248	0.501	0.016	0.021	930.781	

^aHumidity conditions were:

60°C at 100% saturation for first 13 days and 70°C at 98% Relative Humidity for 14 through 123 days. The reason for the variance in test conditions was because the cell specimens were tested piggyback with other specimens on other programs which had priority on the test conditions.

^bI-V test conditions were: AML, 28°C

Table A-14. I-V Test Data After Humidity Tests (Thick Film Ag Paste)^{a,b}

Cumulative No. of Days Exposure to Humidity	Six Cells Total	I _{sc} (mA)	V _{oc} (mV)	P _{mp} (mW)	I _{mp} (mA)	V _{mp} (mV)	Eff (%)	Fill Factor (FF)	R _s (Series Resistance, ohms)	R _{sh} (Shunt Resistance, ohms)	% Change in Cell Efficiency
0	Average	118.822	586.922	34.200	90.344	372.978	8.544	0.487	1.348	95.600	0
	Std. Dev.	4.208	2.531	8.400	11.480	48.286	2.096	0.105	0.529	67.638	
3	Average	114.844	572.733	29.533	82.244	354.044	7.378	0.443	1.535	73.556	-13.65
	Std. Dev.	7.268	22.720	7.065	13.336	37.072	1.762	0.080	0.597	71.679	
13	Average	114.233	578.778	29.778	83.678	350.800	7.444	0.444	1.578	93.822	-12.87
	Std. Dev.	8.293	11.244	7.261	13.712	37.979	1.793	0.083	0.572	118.880	
33	Average	111.450	578.963	29.512	82.675	351.712	7.362	0.452	1.671	126.362	-13.83
	Std. Dev.	7.263	5.036	7.212	12.462	43.084	1.810	0.088	0.716	139.800	
63	Average	110.300	578.375	27.738	79.175	343.925	6.938	0.427	1.879	213.200	-18.80
	Std. Dev.	8.522	3.360	7.777	15.593	36.989	1.940	0.092	0.797	302.839	
123	Average	99.125	577.062	19.075	62.600	302.500	4.750	0.326	3.042	25.938	-44.40
	Std. Dev.	18.693	4.807	5.531	16.877	11.411	1.399	0.044	1.347	14.611	

^aHumidity conditions were: 60°C at 100% saturation for first 13 days and 70°C at 98% Relative Humidity for 14 through 123 days. The reason for the variance in test conditions was because the cell specimens were tested piggyback with other specimens on other programs which had priority on the test conditions.

^bI-V test conditions were: AM1, 28°C

1. Report No. 85-86		2. Government Accession No.		3. Recipient's Catalog No.	
4. Title and Subtitle Environmental Tests of Metallization Systems for Terrestrial Photovoltaic Cells				5. Report Date December 31, 1985	
				6. Performing Organization Code	
7. Author(s) P. Alexander, Jr.				8. Performing Organization Report No.	
9. Performing Organization Name and Address JET PROPULSION LABORATORY California Institute of Technology 4800 Oak Grove Drive Pasadena, California 91109 <i>JIS14450</i>				10. Work Unit No.	
				11. Contract or Grant No. NAS7-918	
				13. Type of Report and Period Covered JPL Publication o	
12. Sponsoring Agency Name and Address NATIONAL AERONAUTICS AND SPACE ADMINISTRATION Washington, D.C. 20546				14. Sponsoring Agency Code	
15. Supplementary Notes Sponsored by the U.S. Department of Energy through Interagency Agreement DE-AI01-76ET20356 with NASA; also identified as DOE/JPL 1012-113 and as JPL Project 5101-280 (RTOP or Customer Code 776-52-61).					
16. Abstract Seven different solar cell metallization systems were subjected to temperature cycling tests and humidity tests. Temperature cycling excursions were -50°C to 150°C per cycle. Humidity conditions were 70°C at 98% relative humidity. The seven metallization systems were: (1) Ti/Ag , (2) Ti/Pd/Ag , (3) Ti/Pd/Cu , (4) Ni/Cu , (5) Pd/Ni/Solder , (6) Cr/Pd/Ag , and (7) Thick Film Ag . All of the seven metallization systems showed slight to moderate decrease in cell efficiencies after subjection to 1000 temperature cycles. Six of the seven metallization systems also evidenced slight increases in cell efficiencies after moderate numbers of cycles, generally less than 100 cycles. The copper-based systems showed the largest decrease in cell efficiencies after temperature cycling. All of the seven metallization systems showed moderate to large decreases in cell efficiencies after 123 days of humidity exposure. The copper-based systems again showed the largest decrease in cell efficiencies after humidity exposure. Graphs of the environmental exposures versus cell efficiencies are presented for each of the metallization systems, as well as environmental exposures versus fill factors or series resistance.					
17. Key Words (Selected by Author(s)) Energy Storage Power Sources Materials solar arrays photovoltaic cells humidity temperature effects metallizing			18. Distribution Statement mass spectroscopy performance tests Unclassified-unlimited cost reduction energy storage graphs (charts) tables (data)		
19. Security Classif. (of this report) Unclassified <i>efficiencies</i>		20. Security Classif. (of this page) Unclassified		21. No. of Pages 88	22. Price